Geoderma 396 (2021) 115073

Contents lists available at ScienceDirect

Geoderma

journal homepage: www.elsevier.com/locate/geoderma

Consequences of chemical pretreatments in particle size analysis for modelling wind erosion

Moritz Koza [a,*], Gerd Schmidt [a], Andrej Bondarovich [b], Kanat Akshalov [c], Christopher Conrad [a], Julia Pöhlitz [a]

[a] Department of Geoecology, Institute of Geosciences and Geography, Martin Luther University Halle-Wittenberg, 06120 Halle (Saale), Germany
[b] Department of Economic Geography and Cartography, Institute of Geography, Altai State University, 656049 Barnaul, Russia
[c] Department of Soil and Crop Management, Barayev Research and Production Center for Grain Farming, 474010 Shortandy, Kazakhstan

ARTICLE INFO

Handling Editor: Morgan Cristine L.S.

Keywords:
Soil texture
Laser diffraction
Hydrochloric acid
Hydrogen peroxide
Wind erosion prediction system
SWEEP
Derivation of soil characteristics

ABSTRACT

The particle size distribution (PSD) of soil plays a vital role in wind erosion prediction. However, the impact of different pretreatments to remove binding agents for PSD and consequences for wind erosion modelling have not been tested. We collected 90 topsoil samples of Chernozems and Kastanozems from different test sites in Kazakhstan. Soil samples covered typical land-use types and farming methods with calcium carbonate contents reaching from 2.2 to 117.3 g kg^{-1} and soil organic carbon content from 11.2 to 48.7 g kg^{-1}. Prior to particle size analysis by laser diffraction, samples were chemically pretreated separately and successively with 10% hydrochloric acid (HCl), to dissolve carbonates and 30% hydrogen peroxide (H_2O_2), to oxidise organic binding material. The HCl pretreatment resulted in incomplete dispersion or even aggregation due to calcium ions released by the dissolution of carbonates, while removing organic matter with H_2O_2 caused complete sample dispersion. The associated changes in PSD were overall minor, and only a few of our samples were assigned to a different texture class. Obtained PSD data was used to calculate texture-based properties, such as the geometric mean diameter (GMD), with a pedotransfer function. Calculated and measured input data were applied to the Single–event Wind Erosion Evaluation Program (SWEEP) to estimate potential soil losses. As a result, SWEEP's simulations showed substantial variations if the GMD is calculated based on PSD under the influence of different pretreatments. At the same time, there was no variation if the GMD was independently measured. We suggest that for standard particle size analysis of calcareous soils, pretreatment with HCl should be avoided because it might cause misleading results. Considering the variation induced by PSD analysis and resulting potential soil losses, pretreatments for laser diffraction analysis can be omitted for the investigated, silt-dominated Chernozems and Kastanozems if additional texture-based parameters are measured.

1. Introduction

Adapting agriculture to climate change is currently one of the most urgent challenges worldwide (Keesstra et al., 2016; UN, 2019; WEF, 2020). The semi-arid steppe regions of Asia suffer from extreme climate conditions and land-use management. This enhances wind and water erosion which causes a loss in soil productivity (Abbas et al., 2020; FAO, 2017; Li et al., 2020; Reyer et al., 2017).

Kazakhstan is one of the world's largest grain exporters (FAO, 2017). It showed its yield potential in 2009 with 2.5% of the world's total wheat (*Triticum* L.) production (FAO, 2012; Sommer et al., 2013). As the largest country in Central Asia, it is the most important grain exporter with potentially up to 84.5 Mio hectares of agricultural land (Almaganbetov and Grigoruk, 2008). However, Kazakhstan is likely a major hotspot of heat stress for wheat in the future climate change scenario A1B (2071–2100) predicted from the baseline climate (1971–2000) (Teixeira et al., 2013). Water scarcity (FAO, 2012) and wind erosion affect agricultural productivity already on about 25.5 Mio hectares (Almaganbetov and Grigoruk, 2008). Counteracting these developments require reliable tools and methods to quantitatively assess soil erosion risk under

Abbreviations: GMD, geometric mean diameter; H_2O_2, hydrogen peroxide; HCl, hydrochloric acid; HCl_{SC}, hydrochloric acid soluble compounds; LDA, laser diffraction analysis; PSD, particle size distribution; SWEEP, Single-event Wind Erosion Evaluation Program.

* Corresponding author.
E-mail address: moritz.koza@geo.uni-halle.de (M. Koza).

https://doi.org/10.1016/j.geoderma.2021.115073
Received 16 December 2020; Received in revised form 22 February 2021; Accepted 1 March 2021
Available online 4 May 2021

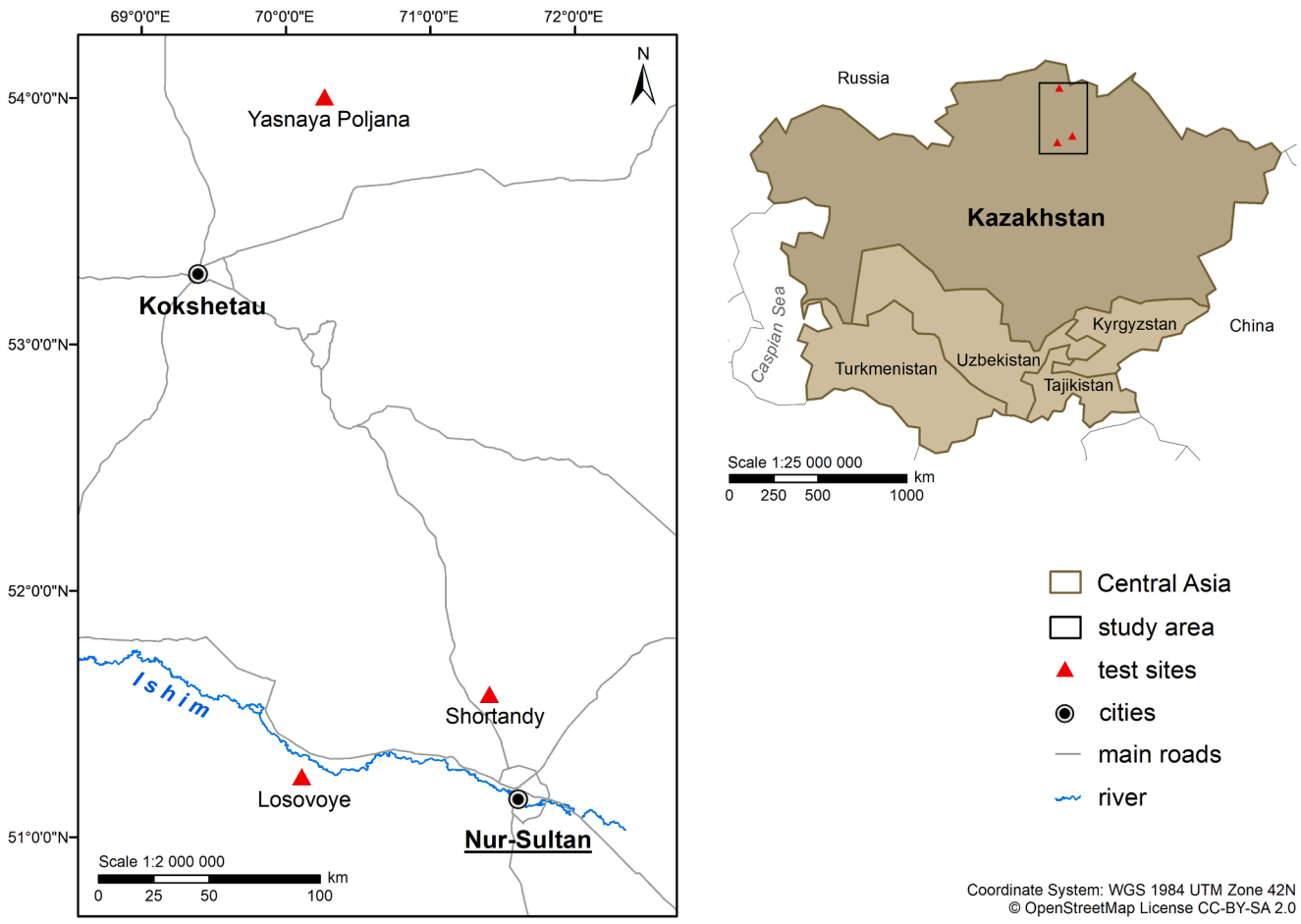

Fig. 1. Geographical location of the study area in Central Asia, including the three test sites in Kazakhstan. The test field for soil loss estimations and the meteorological station are located in Losovoye.

current and future climatic conditions.

Soil texture is a key component of any data set used for implementing sustainable agricultural practices (Kettler et al., 2001). It is one of the primary soil properties affecting the soil's susceptibility to water and wind erosion (Bowker et al., 2008; Zobeck and Van Pelt, 2015). Estimating the loss of soil by water erosion with the Revised Universal Soil Loss Equation (RUSL) requires both information on soil texture and organic matter content to derive the soil erodibility factor (K-factor). In wind erosion models, the percentages of silt, sand, and clay are critical components independent of the models' complexity or capabilities (Jarrah et al., 2020). They are necessary in order to estimate soil loss with the Wind Erosion Prediction System (WEPS) or needed to compute the erodible fraction to apply the Revised Wind Erosion Equation (RWEQ).

Particle size analysis to assign texture classes requires the dispersion of soil aggregates and the removal of binding agents: iron oxide, carbonates, and organic matter (Gee and Or, 2002). Iron oxide coatings are usually not discussed for the topsoil layer in dry steppe biomes. They are just slightly weathered and do not indicate acidity of less than a pH value of six. Carbonates can be removed using hydrochloric acid (HCl). However, decalcification is not a standardized procedure, and this time-consuming pretreatment is often omitted in PSD (ISO 11277, 2002; Schulte et al., 2016). To remove organic matter, hydrogen peroxide (H_2O_2) has been recommended as a standard oxidant for most soils (Gee and Or, 2002; Kroetsch and Wang, 2007). However, all chemical pretreatments could lead to unpredictable effects on particle size distribution (PSD). For instance, HCl does not only remove carbonates but also small amounts of organic matter (Bisutti et al., 2004) and might dissolve poorly ordered metal oxides, too (Carroll and Starkey, 1971). A treatment with H_2O_2 might lead to a disintegration of layered silicates and, when applied to calcareous soils, result in precipitation of calcium oxalate (Mikutta et al., 2005). Currently, there is uncertainty about the consequences of different soil pretreatments on PSD analysis and the subsequent variation in soil erosion estimates.

Therefore, we compared PSD data from non-pretreated soil, soil after two different HCl pretreatments, after H_2O_2 pretreatment, and after sequential H_2O_2 and HCl pretreatment. After each pretreatment, PSD was measured by laser diffraction analysis (LDA). This method has become widely used and accepted in soil science. Laser diffraction is in good agreement with independent optical methods (Bittelli et al., 2019) and has been applied to wind erosion modelling in the past (Pi et al., 2016).

For our experiment, we relied on Chernozem and Kastanozem soils from the dry steppe biome of Kazakhstan. They contain high amounts of organic matter and secondary carbonates (Eckmeier et al., 2007) as binding agents and are also favourable for agriculture. However, their parent material consists of aeolian sediments and is most vulnerable to wind erosion in drylands (Schmidt et al., 2020).

Based on different texture data, we modelled potential soil losses by wind erosion for an arable field in Kazakhstan's dry steppe with the Single-event Wind Erosion Evaluation Program (SWEEP). This submodel of the Wind Erosion Prediction System, the state-of-the-art research and decision-support system to predict wind erosion worldwide, estimates soil losses for a single day storm event under the influence of site-specific input data (Hagen, 1991; Tatarko et al., 2019). Besides texture, texture-based properties, such as the geometric mean

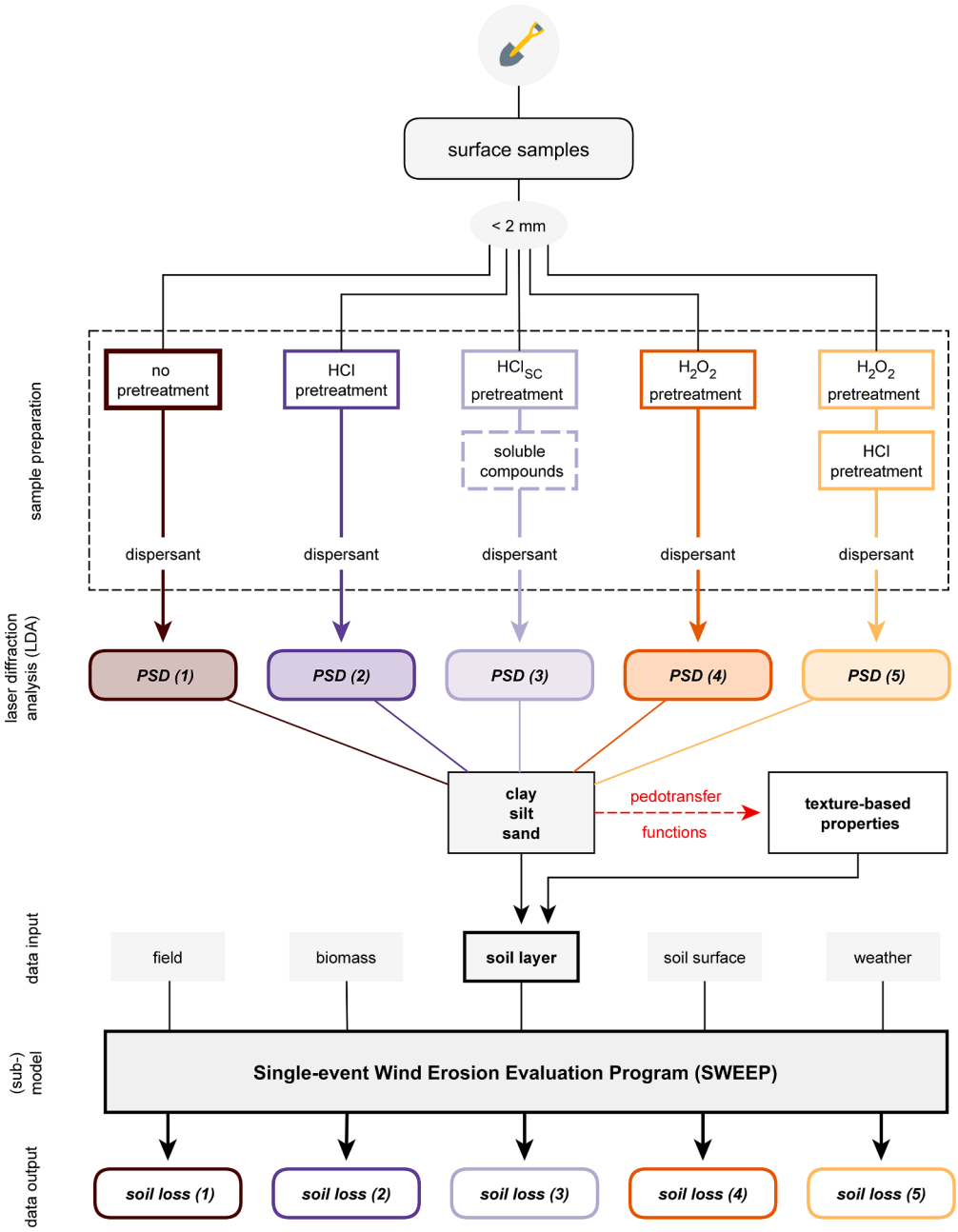

Fig. 2. Hierarchical data structure defining the study design. Sample preparation for measuring particle size distribution (PSD) by laser diffraction included no pretreatment and four different pretreatments, such as hydrochloric acid (HCl) pretreatment, HCl soluble compounds (HCl_{SC}) pretreatment, hydrogen peroxide (H_2O_2) pretreatment and the sequential hydrogen peroxide and hydrochloric acid (H_2O_2 + HCl) pretreatment. Results of PSD were used as data input for the Single–event Wind Erosion Evaluation Program (SWEEP) to estimate soil losses by wind erosion and to calculate texture-based properties with pedotransfer functions from the SWEEP user manual (Tatarko, 2008).

diameter (GMD) and other, are important input data for SWEEP. In case only a minimum of measured parameters are available, these texture-based properties can be derived from PSD with pedotransfer functions.

The main objectives of this study are (i) to compare the effects of different chemical pretreatments on PSD by LDA, (ii) to test the efficiency of pretreatments to remove binding agents, and (iii) to compare modelling estimates of soil loss based on PSD with either calculated or measured GMD.

2. Material and methods

2.1. Study area

The study area is located in the north-eastern part of Kazakhstan, which is mostly flat. The area of interest connects the central and the east-central part of the Eurasian steppe belt. Test sites (Fig. 1) are north of Kokshetau in Yasnaya Poljana (Ясная Поляна: 54°01′11.8″N, 70°15′00.2″E), north of Kazakh's capital Nur-Sultan in Shortandy (Шортанды: 51°34′35.2″N, 71°16′04.3″E) and west at the Ishim River in Losovoye (Лозовое: 51°11′58.9″N, 70°02′06.2″E). All test sites belong administratively to North Kazakhstan and Akmola. Both are provided with water by the Ishim river basin, which has the lowest groundwater reserves in Kazakhstan (FAO, 2012). The study area covers a transect of 300 km with a dry continental climate, following a weak climatic gradient in precipitation and temperature from north to south. The annual precipitation height and mean annual temperature in Yasnaya Poljana are 352.0 mm and 2.8 °C, in Shortandy 327.0 mm and 3.3 °C, and Losovoye 297.8 mm and 3.7 °C (1989–2019) based on weighted interpolation (Harris et al., 2020; Zepner et al., 2020). One-third of the annual precipitation occurs as snowfall. Overall, different types of Chernozem and Kastanozem soils form a heterogeneous pattern in the study area (FAO/UNESCO, 2007; Uspanov et al., 1975). Haplic Chernozems are dominant at the north end of the study area close to Yasnaya Poljana. In Shortandy, Calcic Chernozems and around Losovoye, primarily Calcic Kastanozems exist (Uspanov et al., 1975).

Kazakhstan experienced the most considerable anthropogenic land cover change in the twentieth century. During the 'Virgin Lands Campaign', about 420 000 km^2 of temperate grassland, mainly in northern Kazakhstan and in the Altai region of Russia, were converted into arable land for grain production (Frühauf et al., 2020; Prishchepov et al., 2020). Large areas of arable land were abandoned after the collapse of the Soviet Union in 1991. However, most areas have been reploughed by now. North Kazakhstan and Akmola together with Kostanay comprise the most extensive areas of arable land in Kazakhstan. Grain crops are mainly cultivated, and spring wheat (*Triticum aestivum* L.) is the most common crop. Despite agriculture, there are pastures and native steppes with Stipa (*Stipa capillata* L.), Volga fescue (*Festuca valesiaca* Schleich. ex Gaudin) and shrubs (*Artemisia* spp.) typical (Rachkovskaya and Bragina, 2012).

2.2. Soil sampling

In late May of 2018, we took 90 undisturbed topsoil samples from twelve fields using 250 cm^3 soil sample rings (diameter = 80 mm, height = 50 mm; Eijkelkamp, Giesbeek, Netherlands). A wide range of different land-use types (native steppe, pasture and arable fields) and farming methods were covered, including standard tillage practices such as fallow, deep tillage (with chisel plough), no-till (without tillage), reduced tillage (shallow tillage with a cultivator or disc harrow), diverse tillage (with new farming procedures or machines). Irrigation was not present. Each of the three fields in Yasnaya Poljana were sampled with six topsoil samples. In Shortandy, two fields, and Losovoye, seven fields were sampled with eight topsoil samples each ($n = (3 \times 6) + (9 \times 8) = 90$). Samples on arable fields were taken before they were being sowed. Each field was sampled randomly according to the general agricultural sampling procedure up to 30 cm representing the topsoil layer (Conklin and Meinholtz, 2004). All samples were taken within the A horizon and the depth to where tillage practices extend.

2.3. Physical-chemical soil analysis

Soil samples from field sampling were transferred to plastic bags, air-dried, gently crushed, and dry sieved with a 2-mm sieve. Loose organic material was separated by electrostatics. Each sample (<2 mm) was then adequately split into subsamples (ISO 14488, 2007) for physical-chemical soil analysis.

Soil pH was determined potentiometrically using a glass electrode in a 1:5 suspension of soil in distilled water (ISO 10390, 2005). Electric conductivity was measured at a soil-to-water ratio of 1:2.5 (Sonmez et al., 2008). The calcium carbonate ($CaCO_3$) content was calculated by analysing the carbonate content using a Scheibler calcimeter (Carl Hamm, Essen, Germany). Therefore, the volume of carbon dioxide released after adding 4 M HCl (ISO 10693, 1995) was determined. Total carbon and total nitrogen were determined after high-temperature combustion of 1 g soil by 950 °C using an elemental analyser (vario Max Cube, Elementar, Langenselbold, Germany). Soil organic carbon was calculated from total carbon and calcium carbonate (organic carbon = total carbon − 0.12 × calcium carbonate). Organic matter was estimated from organic carbon by the factor 1.72 (FAO, 2006).

2.4. Particle size analysis

2.4.1. Sample preparation

For particle size analysis, subsamples were exposed to the following pretreatments (Fig. 2):

no pretreatment: 2 ml of 0.05 M sodium pyrophosphate ($Na_4P_2O_7 \times 10\ H_2O$) solution was added as the dispersion medium to 10-g soil. The soil turned to a 'paste-like' consistency as required for LDA (ISO 13320, 2009).

HCl pretreatment: 25 ml of deionised water was added to 10-g soil. For each percentage of carbonate, 1 ml of 10% HCl was added dropwise until pH decreased between 4.0 and 4.5, resulting in a maximal volume of 70 ml. Afterwards, the suspension was kept on a heating plate at 50 °C until the reaction ceased completely. After removing the clear supernatant, the dispersion medium was added as described above.

HCl soluble compounds (HCl_{SC}) pretreatment: 10-g soil was pretreated as mentioned before. Following the HCl treatment, the recovered soil was resuspended in deionised water between 500 and 3000 ml until the electric conductivity in the clear supernatant turned < 500 µS/cm. After removing the supernatant, the dispersion medium was added.

H_2O_2 pretreatment: 10-g soil was pretreated with 30% H_2O_2. Each time, 15 ml H_2O_2 was added to avoid excessive foam production, and no more than 100 ml H_2O_2 was applied. After the initial reaction ceased, the suspension was kept for one hour on a heating plate at 50 °C. Afterwards, the suspension was allowed to settle and the clear supernatant removed with a pipette. The dispersion medium was added.

H_2O_2 + HCl pretreatment: 10-g soil was sequentially pretreated with H_2O_2 and HCl as described above but without washing out soluble compounds. The dispersion medium was added.

2.4.2. Laser diffraction analysis

The PSD was measured with a laser diffraction analyser (Helos/KR, Sympatec GmbH, Clausthal-Zellerfeld, Germany) equipped with a 60 W sonotrode and a fully automated wet dispersion unit of 1000 ml water (Quixel, Sympatec GmbH, Clausthal-Zellerfeld, Germany). A second replicate was measured to ensure the first measurement. The diffraction system uses a helium-neon laser light source (wavelength = 632.8 nm) with fibre optical cable and a fixed beam expansion unit (Sympatec, 2012). It has an accuracy of ± 1%, a precision of < 0.04%, and comparability from one system to another of < 1% (Sympatec, 2019). It does not merge laser diffraction and light scattering and determines 49 physical particle size classes ranging from 0.5 to 3500 µm.

Table 1
Single-event Wind Erosion Evaluation Program (SWEEP) input parameters and values for modelling wind erosion on the 29th of April 2019 on a fallow arable test field in Losovoye. Values were measured, assumed, estimated or calculated following the SWEEP user manual (Tatarko, 2008).

SWEEP	parameter	source	value
Field	x lenght, y length [m]	estimated	2000.00
	angle from north [°]	assumed	0.00
	wind barriers	estimated	*none*
Biomass	residue average height [m]	assumed	0.00
	residue stem area index [m^2 m^{-2}]	assumed	0.00
	residue leaf area index [m^2 m^{-2}]	assumed	0.00
	residue flat cover [m^2 m^{-2}]	estimated	0.30
	growing crop average height [m]	assumed	0.00
	growing crop stem area index [m^2 m^{-2}]	assumed	0.00
	growing crop leaf area index [m^2 m^{-2}]	assumed	0.00
	row spacing [m]	assumed	0.00
	seed placement	estimated	*furrow*
Soil layer	number of layers	measured	1.00
	thickness [mm]	measured	300.00
	sand fraction [kg kg^{-1}]	measured *	0.08–0.14
	very fine sand fraction [kg kg^{-1}]	measured *	0.06–0.11
	silt fraction [kg kg^{-1}]	measured *	0.69–0.79
	clay fraction (<2 μm) [kg kg^{-1}]	measured *	0.07–0.19
	rock volume fraction [m^3 m^{-3}]	assumed	0.00
	dry bulk density [kg m^{-3}]	measured	1.09
	average aggregate density [kg m^{-3}]	calculated	1.46
	average dry aggregate stability [ln(J kg^{-1})]	calculated	1.80–2.98
	geometric mean diameter [mm]	calculated **	4.15–5.30
	geometric standard deviation [mm mm^{-1}]	calculated	15.47–15.96
	minimum aggregate size [mm]	estimated	0.01
	maximum aggregate size [mm]	estimated	14.84–18.86
	soil wilting point water content [kg kg^{-1}]	measured	0.15
Soil surface	surface crust fraction [m^2 m^{-2}]	assumed	0.00
	surface crust thickness [m m^{-1}]	assumed	0.00
	loose material on crust [m^2 m^{-2}]	assumed	0.00
	loose mass on crust [kg m^{-2}]	assumed	0.00
	crust density [kg m^{-3}]	calculated	1.46
	crust stability [ln(J kg^{-1})]	calculated	1.80–2.98
	allmaras random roughness [mm]	estimated	10.00
	ridge height [mm]	assumed	0.00
	ridge spacing [mm]	estimated	300.00
	ridge width [mm]	estimated	100.00
	ridge orientation from north [°]	assumed	0.00
	dike spacing [mm]	assumed	0.00
	snow depth [mm]	assumed	0.00
	hourly surface water content [kg kg^{-1}]	assumed	0.00
Weather	air density [kg m^{-3}]	calculated	1.18
	wind direction from north [°]	measured	250.8
	anemometer height [m]	measured	2.00
	wind speed (max) [m s^{-1}]	measured	Fig. 3

* data input varies depending on pretreatment of particle size analysis by LDA (Table 2 and Table 3).

** data input first derived from soil texture and calculated (Table 2), then measured (Table 3).

In laser diffraction, particles scatter light with different intensities according to their size in the near forward direction. The diffraction of light by a single particle is described mathematically by the Fraunhofer theory because it applies to mixtures of different materials. No optical properties, such as each particle's refractive index, are required (Green and Perry, 2007; ISO 13320, 2009). Particle size analysis was applied to 2–3 g of soil for 20 sec after 1 min of 60 W sonicating. During laser diffraction, the extent of obscuration was always between 20 and 30%. Based on the United States Department of Agriculture (USDA), eight particle size subclasses were used to present PSD data between 0.5 and 2000 μm (Soil Science Division Staff, 2017). The used 2–50–2000 μm particle size classification system is currently most common in wind erosion and land-surface modelling (Shao, 2008).

Table 2
The data input of clay [kg kg^{-1}], silt [kg kg^{-1}], sand [kg kg^{-1}] and very fine sand [kg kg^{-1}] were measured by laser diffraction analysis. The geometric mean diameter of aggregate sizes [mm], average dry aggregate stability [ln(J kg^{-1})], geometric standard deviation of aggregate sizes [mm] and maximum aggregate size [mm] derived from results of laser diffraction analysis following the SWEEP user manual (Tatarko, 2008). Estimates of soil losses for a fallow arable test field in Losovoye are shown as data output. Total soil loss [kg m^{-2}] consists of saltation and creep loss [kg m^{-2}] and suspension loss [kg m^{-2}]. The fine particulate matter of 10 μm or less in diameter (PM_{10}) [kg m^{-2}] is part of the suspension loss.

	data input SWEEP measured (laser diffraction analysis)				estimated (derived values by pedotransfer functions)				data output SWEEP simulated			
	clay	silt	sand	very fine sand	geometric mean diameter of aggregate sizes	average dry aggregate stability*	geometric standard deviation of aggregate sizes	max. aggregate size	total soil loss	saltation/ creep loss	suspension loss	PM_{10} loss
	[kg kg^{-1}]	[kg kg^{-1}]	[kg kg^{-1}]	[kg kg^{-1}]	[mm]	[ln(J kg^{-1})]*	[mm mm^{-1}]	[mm]	[kg m^{-2}]	[kg m^{-2}]	[kg m^{-2}]	[kg m^{-2}]
no pretreatment	0.16	0.72	0.12	0.09	4.84	2.71	15.80	17.15	5.717	0.887	4.830	0.175
HCl pretreatment	0.07	0.79	0.14	0.11	4.15	1.80	15.47	14.84	12.858	0.885	11.973	0.643
HCl_{SC} pretreatment	0.13	0.74	0.13	0.09	4.60	2.48	15.70	16.35	7.904	0.995	6.908	0.255
H_2O_2 pretreatment	0.19	0.74	0.08	0.06	5.30	2.94	15.96	18.68	3.753	0.730	3.022	0.112
H_2O_2 + HCl pretreatment	0.19	0.69	0.11	0.08	5.11	2.98	15.90	18.04	3.595	0.732	2.863	0.106

* average dry aggregate stability is also used as an estimate for crust stability (Tatarko, 2008).

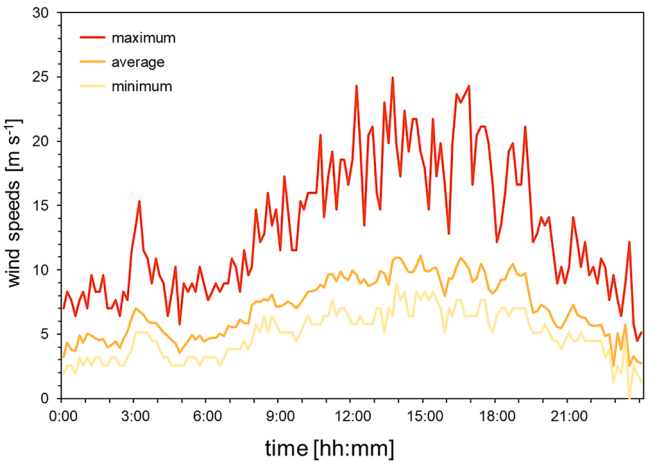

Fig. 3. Wind speeds [m s^{-1}] on the 29th of April 2019 from the meteorological station in Losovoye. The data consists of 10-min wind speed averages, minima and maxima. Wind speed maxima were used for modelling wind erosion following the SWEEP user manual (Tatarko, 2008).

2.5. Wind erosion modelling

2.5.1. Test site for wind erosion modelling

The wind erosion model was set up for 24 h on the 29th of April 2019 for a test field in Losovoye (51°11′11.2″N, 70°04′13.3″E), which has been cultivated with a deep tillage chisel plough (<300 mm) since 2010. This area's prevalent soil type was identified as a dark chestnut calcareous soil (Uspanov et al., 1975), which corresponds to a Calcic Kastanozem (Stolbovoi, 2000). The field size is about 2000 × 2000 m, a standard field size for the study area. There was no wind barrier to protect the test field. The test field was to be sowed on the 20th of May and fallow that day.

A meteorological station of about 6 km from the test site measured weather data (51°14′12.3″N, 70°04′09.8″E) and provided 10-min averages. The day's average wind speed was 7.06 m s^{-1}. The highest measured wind speed (v_{max} = 24.96 m s^{-1}) in 2019, while topsoil was not frozen, was recorded that day. The day's average temperature was 15.4 °C, and there was no precipitation measured.

Overall soil physics, agricultural implementations as well as weather parameters were predestined for a wind erosion event.

2.5.2. Single-event wind erosion evaluation program (SWEEP)

The process-based computer model SWEEP (Version 1.5.52, USDA-ARS, Manhattan/Kansas, USA) was used to simulate soil loss by wind erosion on the test site. The open-source model provides easy access to in- and outputs for a single-day storm event (Jarrah et al., 2020) and has been extensively validated worldwide (Tatarko et al., 2016). The SWEEP computes soil loss and deposition of a specific test site with particular field size and orientation in response to wind speed, wind direction, and surface conditions on a sub-hourly basis. The model determines first the threshold friction velocity at which erosion begins. Then, it calculates when the aerodynamic forces (aerodynamic drag and the aerodynamic lift) overcome the retarding forces of the surface particles (gravity force and the inter-particle cohesive force). In the final step, it simulates multiple physical erosion processes for each surface condition (Shao, 2008; Tatarko, 2008). The threshold is calculated based on different input parameters regarding biomass, soil layer, soil surface, and weather. Once wind speed exceeds the threshold, it calculates soil losses over a series of individual grid cells representing the field. To evaluate off-site impacts, the model's outcome of total soil loss in kg m^{-2} is divided in saltation plus creep and suspension loss. Fine particulate matter of 10 μm or less in diameter (PM_{10}) is also identified as part of suspension (Tatarko, 2008).

The Wind Erosion Prediction System has been developed initially for soils with organic matter content of less than 0.03 kg kg^{-1} (Tatarko, 2020). The test field with an average organic matter content of 0.025 kg kg^{-1} could be applied to SWEEP. All input parameters of the test field are shown in Table 1.

Field: Because of the extensive field size, the number of grids was increased manually to 400×400 cells. The discretisation of SWEEP depends on the erosion activity in each grid cell, which should be downsized by increasing soil surface processes. However, it should generally be at least 7×7 m.

Biomass: Input parameters regarding biomass could be mostly omitted because the test site was fallow. Residue flat cover, described as the flat biomass cover [m^2 m^{-2}], was minimal and could be estimated with photo examples from the SWEEP user manual (Tatarko, 2008).

Soil layer: Quantities of clay (<2 μm [kg kg^{-1}]), silt (2–50 μm [kg kg^{-1}]), sand (50–2000 μm [kg kg^{-1}]) and of the subclass very fine sand (50–100 μm [kg kg^{-1}]) from LDA were used. The test sites average was used as input data and varied depending on PSD pretreatment (see * Table 1 and Table 2). To reduce the uncertainty of missing data, assumptions were made carefully by considering all available information. Estimates were used from the SWEEP user manual (Tatarko, 2008), including all equations to derive texture-based properties. In-depth descriptions of the used functions are explained in the Technical Documentation (Tatarko, 2020).

The average aggregate density is the oven-dry weight of soil aggregates (<2 mm) per unit volume of dry soil aggregates [kg m^{-3}]. It was calculated using the method of Rawls (1983) from the SWEEP user manual (Eq. (1)).

$$aggregate\ density = 2.01 \times (0.72 + 0.00092 \times layer\ depth) \quad (1)$$

with,

layer depth is described as the bottom depth of the layer [mm].

The average aggregate stability is described as the mean of the natural logarithm of aggregates crushing energy [ln(J kg^{-1})] (Eq. (2)).

$$aggregate\ stability = 0.83 + 15.7 \times clay - 23.8 \times clay^2 \quad (2)$$

The GMD was calculated directly from PSD and test fields average content of organic matter (0.025 kg kg^{-1}) and calcium carbonate (0.074 kg kg^{-1}) (Eq. (3)).with,

$$GMD = exp(1.343 - 2.235 \times sand - 1.226 \times silt - 0.0238 \times sand/clay + 33.6 \times organic\ matter + 6.85 \times calcium\ carbonate) \times (1 + 0.006 \times surface\ layer\ depth) \quad (3)$$

surface layer depth is 10 mm, and the sand, silt and clay fractions

were measured under the influence of different pretreatments (Table 2).

The averaged GMD was utilised to calculate the geometric standard deviation (Eq. (4)) and the maximum aggregate size (Eq. (5)).

$$Geometric\ \ standard\ deviation = 1/(0.0203 + 0.00193 \times GMD + 0.074/GMD^{0.5}) \quad (4)$$

$$Max.\ \ aggregate\ size = geometric\ standard\ deviation^{p} \times\ GMD\ + 0.84 \quad (5)$$

with, $p = 1.52 \times geometric\ standard\ deviation^{-0.449}$

Soil surface: Event-based input data such as crust density and crust stability were estimated by applying aggregate density and aggregate stability values. Allmaras random roughness was estimated following the pin-type profile meter (Allmaras et al., 1966) via photo examples from the user manual. Surface water content could be omitted based on meterological data.

Weather: One hundred and forty-four measured values of wind speed were applied. Following SWEEP's advice, the maximum wind speed for each 10-min period (Fig. 3) and the mean wind direction (250.8°) was used as data input. Aerodynamic roughness was automatically ignored by SWEEP because wind speeds were measured at anemometer site under field conditions. Air density was estimated by SWEEP itself based on elevation (335 m) and the day's average temperature.

2.5.3. Geometric mean diameter

To improve modelling results, the GMD (Table 1), was determined by fitting the measured mass percentage of different aggregate sizes to a log-normal function (Gardner, 1956; Larney, 2007). Therefore, a horizontal sieve apparatus (Analysette 3, Fritsch GmbH, Idar-Oberstein, Germany) with eight different sieves (8 mm, 5 mm, 3 mm, 2 mm, 0.85 mm, 0.5 mm, 0.25 mm, and 0.05 mm) was applied for 1 min with an amplitude of 1 mm to four samples from the test field. The GMD was then utilised to derive the geometric standard deviation and the maximum aggregate size with pedotransfer functions (Eqs. (4) and (5)) and used for modelling erosion losses (Table 3).

2.6. Statistical analysis

The open-source software 'RStudio' (Version 1.2.5019, RStudio Team, Boston, USA) as an integrated development environment for 'R' was used to perform statistical analysis and graphical illustrations of LDA results (R Core Team, 2020; RStudio Team, 2020). Texture classes and texture triangles were computed and illustrated with the 'soiltexture' package (Moeys, 2018).

Statistical analyses were carried out for each field and each test site. In Yasnaya Poljana each test site is represented by the average of six measured values, and the average mean of test sites in Shortandy and Losovoye consisted of eight values. All parameters, including LDA results of different parameters, were tested for normal distribution (Shapiro–Wilk test) and variance homogeneity (Levene's test) followed by variance analyses (one-way ANOVA). Tukey's range test was used to identify mean group values that are significantly different ($p \leq 0.05$) and are presented in Appendixes Table A1 and Table B1.

3. Results

3.1. Effect of pretreatments on texture class

The results of LDA showed that samples from the study area were predominantly assigned to the texture class silt loam (Soil Science Division Staff, 2017). Pretreatments for PSD did not influence the assigned texture class (Fig. 4). Silt loam consists of more than 50% silt and between 12 and 27% clay or between 50 and 80% silt and less than 12% clay.

Nevertheless, exceptions were assigned to adjacent texture classes depending on the pretreatment used. All samples with no pretreatment were assigned to silt loam (Fig. 4(1)). In comparison, one-third of HCl pretreated samples (Fig. 4(2)) showed a low amount of clay content (between 5 and 9%) and a high amount of silt content (>80%) and were therefore assigned to silt. Results of HCl_{SC} pretreatment (Fig. 4(3)) assigned three out of 90 samples as silt (>80% silt content). The H_2O_2 pretreatment (Fig. 4(4)) assigned one sample as loam because of its low silt content (49%) and one as silty clay loam as a result of high clay content (30%). Following the results of H_2O_2 + HCl pretreatment (Fig. 4 (5)), only one sample was assigned as silty clay loam (28% clay content).

Even though silt loam is the dominant texture class for all pretreatments, the distribution of results within one class varies for each method. The HCl pretreatment results (Fig. 4(2)) show a low scatter, while pretreatments including H_2O_2 (Fig. 4(4) and 4(5)) result in a higher scattering. Data of averaged clay, silt, and sand fractions for each test field are shown in Appendix Table A1.

3.2. Effect of pretreatments on particle size distribution

The averaged cumulative distribution curves of the different pretreatments are shown in Fig. 5. Each curve represents one pretreatment and consists of 40 physically measured classes. Values shown are the averages of all samples. The curves order was mainly the same on all three test sites and under all typical land-use types. Pretreating samples with H_2O_2 generated the highest dispersion (Fig. 5(4)) while pretreating additionally with HCl afterwards did not cause further dispersion for most fields. Only two fields in Yasnaya Poljana (pasture and arable land) showed further breakdown into smaller particles with H_2O_2 + HCl pretreatment. On average, samples with no pretreatment were slightly better dispersed than samples pretreated with HCl_{SC}. Contrary, HCl pretreatment had the opposite effect, and PSD shifted into coarser sizes (Fig. 5(2)).

The scatterplots in Fig. 6 show the effects of pretreatment on PSD for all samples. Comparing the two different HCl pretreatments with no pretreatment showed that percentages of clay, silt, and sand were similar between no pretreatment and HCl_{SC} pretreatment (Fig. 6A). In contrast to HCl pretreatment (Fig. 6B), the amount of silt increases and clay drastically decreases. Samples with no pretreatment showed between 8 and 20% of clay but only between 5 and 9% after pretreating with HCl. Comparing H_2O_2 pretreatment and H_2O_2 + HCl pretreatment revealed no drastic shift between particle classes (Fig. 6C). Measured values are close to the 1:1 line for both methods. Primary dispersion is already seen in samples pretreated with only H_2O_2 in comparison to samples with no pretreatment. The H_2O_2 pretreatment increases the amount of clay and decreases the sand and silt fraction (Fig. 6D).

3.3. Influence of calcium carbonate content on HCl pretreatment

The calcium carbonate content in the study area spanned for the single measured samples from 2.2 to 117.3 g kg^{-1} with an average of 32.5 g kg^{-1} for all Chernozem and 52.6 g kg^{-1} for all Kastanozem samples. Overall, arable fields had a higher content of calcium carbonate on average (56.5 g kg^{-1}) than uncultivated fields (27.9 g kg^{-1}) (Appendix Table B1).

The content of calcium carbonate affected PSD if pretreated with HCl and had no effect if pretreated with HCl_{SC} (data not shown). The HCl pretreatment mainly changed the relative amount of coarse and fine silt minimal. Samples pretreated with HCl tended to increase the coarse silt fraction while the fine silt and coarse clay fraction decreased. The difference between HCl pretreatment and no pretreatment for samples with high calcium carbonate content was not as distinct as the difference between no pretreatment and H_2O_2 pretreatment for samples with high organic carbon content.

Table 3
Measured data input of clay [kg kg^{-1}], silt [kg kg^{-1}], sand [kg kg^{-1}], very fine sand [kg kg^{-1}] and geometric mean diameter of aggregate sizes [mm]. Average dry aggregate stability [ln(J kg^{-1})] was derived from clay content. Geometric standard deviation of aggregate sizes [mm] and maximum aggregate size [mm] were derived from measured GMD following the SWEEP user manual (Tatarko, 2008). Estimates of soil losses for a fallow arable test field in Losovoye are shown as data output. Total soil loss [kg m^{-2}] consists of saltation and creep loss [kg m^{-2}] and suspension loss [kg m^{-2}]. The fine particulate matter of 10 μm or less in diameter (PM_{10}) [kg m^{-2}] is part of the suspension loss.

	data input SWEEP measured (laser diffraction analysis)				measured (dry sieving)	estimated (derived values by pedotransfer functions)			data output SWEEP simulated			
	clay	silt	sand	very fine sand	geometric mean diameter of aggregate sizes	average dry aggregate stability*	geometric standard deviation of aggregate sizes	max. aggregate size	total soil loss	saltation/ creep loss	suspension loss	PM_{10} loss
	[kg kg^{-1}]	[kg kg^{-1}]	[kg kg^{-1}]	[kg kg^{-1}]	[mm]	[ln(J kg^{-1})]*	[mm mm^{-1}]	[mm]	[kg m^{-2}]	[kg m^{-2}]	[kg m^{-2}]	[kg m^{-2}]
no pretreatment	0.16	0.72	0.12	0.09	1.18	2.58	11.03	4.93	10.125	1.114	9.011	0.317
HCl pretreatment	0.07	0.79	0.14	0.11	1.18	2.58	11.03	4.93	9.561	1.020	8.541	0.442
HCl_{SC} pretreatment	0.13	0.74	0.13	0.09	1.18	2.58	11.03	4.93	10.243	1.139	9.104	0.325
H_2O_2 pretreatment	0.19	0.74	0.08	0.06	1.18	2.58	11.03	4.93	9.852	1.064	8.788	0.316
H_2O_2 + HCl pretreatment	0.19	0.69	0.11	0.08	1.18	2.58	11.03	4.93	9.927	1.080	8.847	0.318

* average dry aggregate stability is also used as an estimate for crust stability (Tatarko, 2008).

3.4. Influence of organic carbon content on H_2O_2 pretreatment

The organic carbon content in the study area reached for the single measured samples from 11.2 to 48.7 g kg^{-1} with an average of 29.5 g kg^{-1} for all Chernozem and 16.3 g kg^{-1} for all Kastanozem samples. Overall, arable fields had a lower content of organic carbon on average (17.7 g kg^{-1}) than uncultivated fields (26.6 g kg^{-1}) (Appendix Table B1).

The effect of H_2O_2 pretreatment depends on organic carbon content and affects texture subclasses differently (Fig. 7).

In comparison to HCl pretreatment effects (see 3.3), results of H_2O_2 pretreatment showed the opposite effect. There was no difference between no pretreatment and H_2O_2 pretreatment for particle sizes above 100 μm (data not shown). However, H_2O_2 pretreatment decreased particles of very fine sand (50–100 μm) and coarse silt (20–50 μm) (Fig. 7A and B) in comparison to no pretreatment. The H_2O_2 pretreatment causes an increase of particles in the fine silt (2–20 μm) and coarse clay (0.2–2 μm) subclasses (Fig. 7C and D). Additionally, differences within subclasses between no pretreatment and H_2O_2 pretreatment rely upon the amount of organic carbon. While the sample with the lowest organic carbon content led to a small difference in the coarse silt fraction between no pretreatment (22%) and H_2O_2 pretreatment (14%), the sample with the highest organic carbon content caused a considerable difference between no pretreatment (26%) and H_2O_2 pretreatment (8%). This behaviour applies contrary to the fine silt fraction.

The mentioned effects of organic carbon on H_2O_2 pretreatment were similar to H_2O_2 + HCl pretreatment (data not shown).

3.5. Simulated soil loss using SWEEP

3.5.1. Impact of PSD pretreatments on derived properties

The PSD (Table 2) of different pretreatments from the test field in Losovoye ranged for clay from 0.07 to 0.19 kg kg^{-1}, silt from 0.69 to 0.79 kg kg^{-1}, and sand from 0.08 to 0.14 kg kg^{-1}. The very fine sand subclass ranged from 0.06 to 0.11 kg kg^{-1}. Pretreatments with H_2O_2 led to the highest amount of clay (0.19 kg kg^{-1}) and the lowest amount of very fine sand (0.06 kg kg^{-1}). In comparison, HCl pretreatment led to the highest amount of very fine sand (0.11 kg kg^{-1}) and the lowest amount of clay (0.07 kg kg^{-1}).

Calculated values of aggregate stability reached from 1.80 to 2.98 ln (J kg^{-1}), the GMD from 4.15 to 5.30 mm, the geometric standard deviation from 15.47 to 15.96 mm mm^{-1}, and the maximum aggregate size from 14.84 to 18.68 mm (Table 2). Modelling results were diverse if PSD under the impact of different pretreatments was used to estimate texture-based properties to model wind erosion.

SWEEP simulated a total soil loss between 3.595 kg m^{-2} for H_2O_2 + HCl pretreatment and 12.858 kg m^{-2} for HCl pretreatment. It further simulated the lowest soil losses for H_2O_2 pretreatment, regardless of whether HCl was used or not. If PSD with no pretreatment was used to calculate derived properties, SWEEP simulated a total soil loss of 5.717 kg m^{-2}. Overall, the largest part of total soil loss was due to suspension. The no pretreatment and HCl pretreatment estimates were similar for the saltation/creep loss (0.887 and 0.885 kg m^{-2}). However, they differed for soil loss by suspension (4.830 and 11.973 kg m^{-2}).

Because H_2O_2 pretreatment removed particle binding agents most efficiently, the potential total soil loss estimate simulated by SWEEP (3.753 kg m^{-2}) is shown for the test field in Fig. 8A. All texture-based properties were calculated from PSD data (including H_2O_2 pretreatment). The simulation of soil loss due to saltation and creep movement (0.730 kg m^{-2}) is visualised in Fig. 8B.

3.5.2. Impact of PSD pretreatment on potential soil loss

For the case that PSD and GMD were independently measured, and additional texture-based properties were used as steady estimates, SWEEP simulated a possible total soil loss between 9.561 and 10.243 kg m^{-2}, depending on pretreatments used for LDA

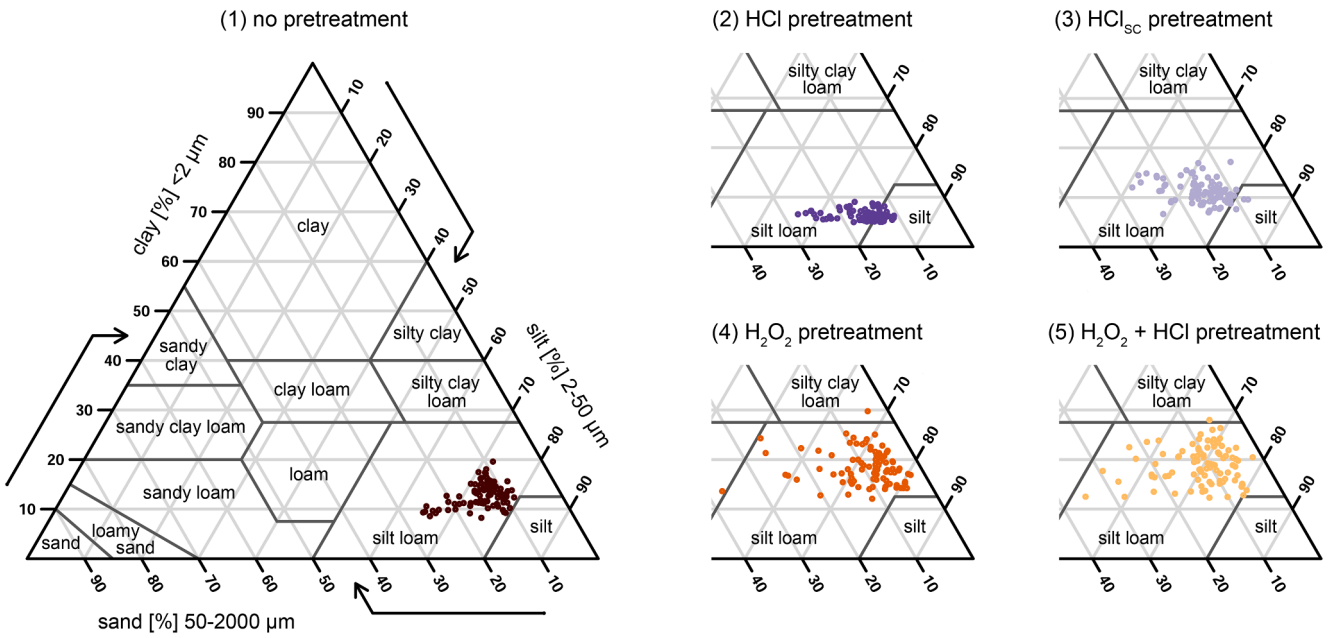

Fig. 4. Soil texture triangles (Soil Science Division Staff, 2017) defining texture classes for all samples (n = 90) depending on different pretreatments: (1) no pretreatment, (2) hydrochloric acid (HCl) pretreatment, (3) hydrochloric acid soluble compounds (HCl_{SC}) pretreatment, (4) hydrogen peroxide (H_2O_2) pretreatment, (5) sequential hydrogen peroxide and hydrochloric acid (H_2O_2 + HCl) pretreatment. Texture classes were assigned from clay, silt and sand fractions measured by laser diffraction analysis (LDA).

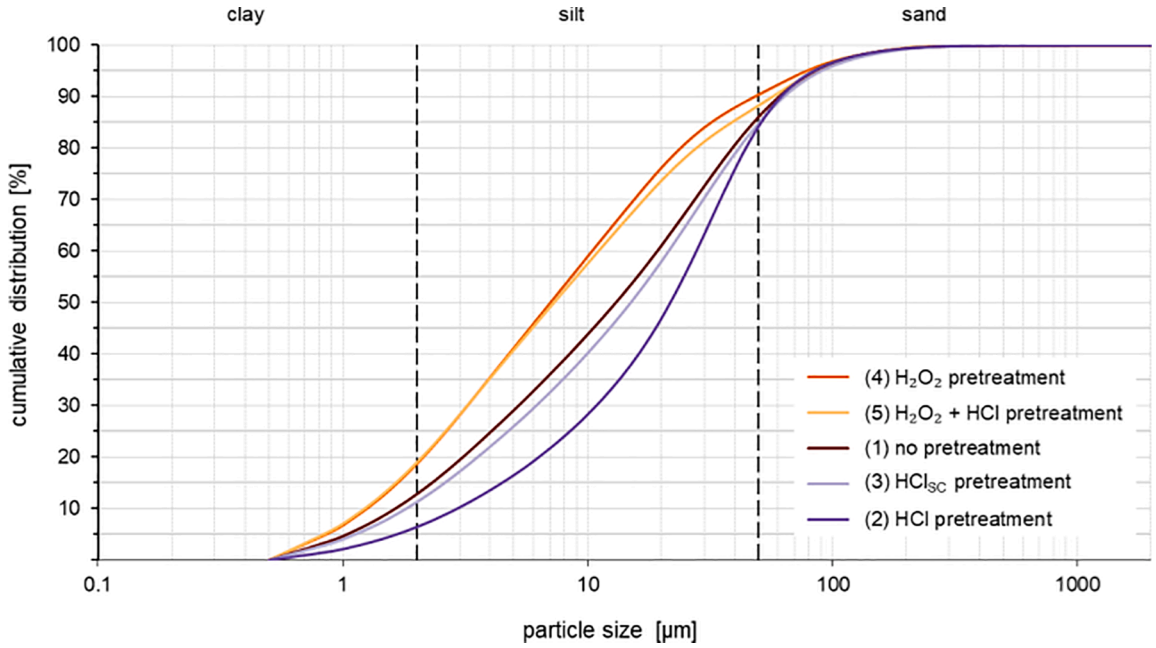

Fig. 5. Cumulative distribution of particle size analysis by laser diffraction (logarithmic scale) depending on pretreatment: (1) no pretreatment, (2) hydrochloric acid (HCl) pretreatment, (3) hydrochloric acid soluble compounds (HCl_{SC}) pretreatment, (4) hydrogen peroxide (H_2O_2) pretreatment, (5) sequential hydrogen peroxide and hydrochloric acid (H_2O_2 + HCl) pretreatment. Data shown represent averages of all samples (n = 90). The laser diffraction analyser measured 40 physical classes up to 100% cumulative distribution.

(Table 3). Pretreatments of particle size analysis did not affect SWEEP's output severely. From the total soil loss, only 1.020–1.139 kg m^{-2} of soil were lost through saltation and creep movement, while most soil was lost due to suspension (8.847–9.104 kg m^{-2}).

Comparison between calculated and measured GMD for modelling results are shown in Fig. 8. Measured PSD (including H_2O_2 pretreatment) and measured GMD was used to simulate potential soil losses with SWEEP. Visualisations of the total soil loss (9.852 kg m^{-2}, Fig. 8C) and saltation and creep loss (1.064 kg m^{-2}, Fig. 8D) are shown.

4. Discussion

4.1. Efficiency of pretreatments to remove carbonates

The dominant occurrence of silt loam in the study area results from the same parent material loess, which is an aeolian and reworked

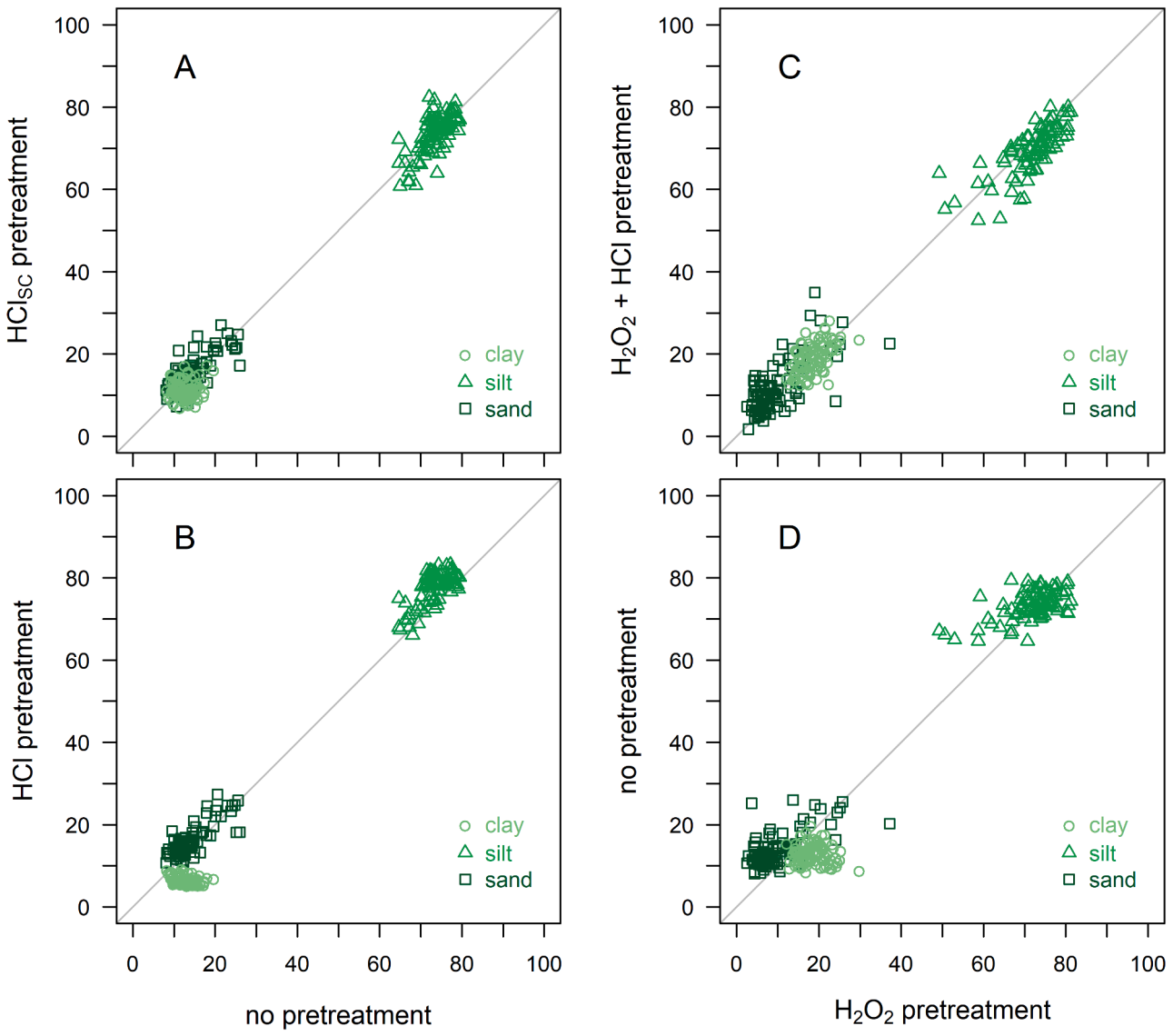

Fig. 6. Scatter plots of cumulative particle size [%] comparing the clay (○), silt (Δ) and sand (□) fractions between different pretreatments. On the left side, results of (A) hydrochloric acid soluble compounds (HCl_{SC}) pretreatment and (B) hydrochloric acid (HCl) pretreatment are compared to no pretreatment. On the right side, differences between (C) the sequential hydrogen peroxide and the hydrochloric acid (H_2O_2 + HCl) pretreatment and (D) no pretreatment are compared to the hydrogen peroxide pretreatment (H_2O_2). The grey line corresponds to the 1:1 line.

aeolian carbonaceous sediment. Chernozems and Kastanozems of the study area are located within the Russian loess belt (Muhs et al., 2014) and experience similar soil pedogenesis. The high concentration of secondary carbonates usually starts in Chernozem soils within 50 cm, at the lower limit of the A horizon (Eckmeier et al., 2007).

In our study, HCl pretreatments caused incomplete dispersion. Schulte et al. (2016) observed that HCl pretreatment is particularly selective and inscrutable. Adding plain HCl to samples dissociates carbonates and may cause a cationic bridging effect of the calcium ions (Ca^{2+}). In that case, carbonates act as an abundant source of calcium ions due to HCl pretreatment. Calcium ions favour inter-molecular interactions between clay and organic matter to form a covalent bond (Rowley et al., 2018; Six et al., 2004; Virto et al., 2011; Wuddivira and Camps-Roach, 2007). The mechanism behind this stabilisation is the flocculation of negatively charged separates by outer-sphere interactions. If samples are already pretreated with H_2O_2, and organic matter is oxidised, the described effect does not occur for Kastanozem soils. Only Chernozem soils of Yasnaya Poljana, with the high organic carbon content and the low carbonate content, showed a slight increase in smaller particles if pretreated with H_2O_2 + HCl. Reasons could be HCl's selective character during pretreatment, or that HCl is already affecting mineral compounds. In case the soil is pretreated with HCl and soluble compounds are washed out, particles remain similar in size. Pretreatments with HCl did not dissolve aggregates, had no considerable effect or even caused aggregation. Carbonates are not the primary binding agent between particles in our study. We would advise avoiding decalcification of Chernozems and Kastanozems because it might lead to unpredictable effects.

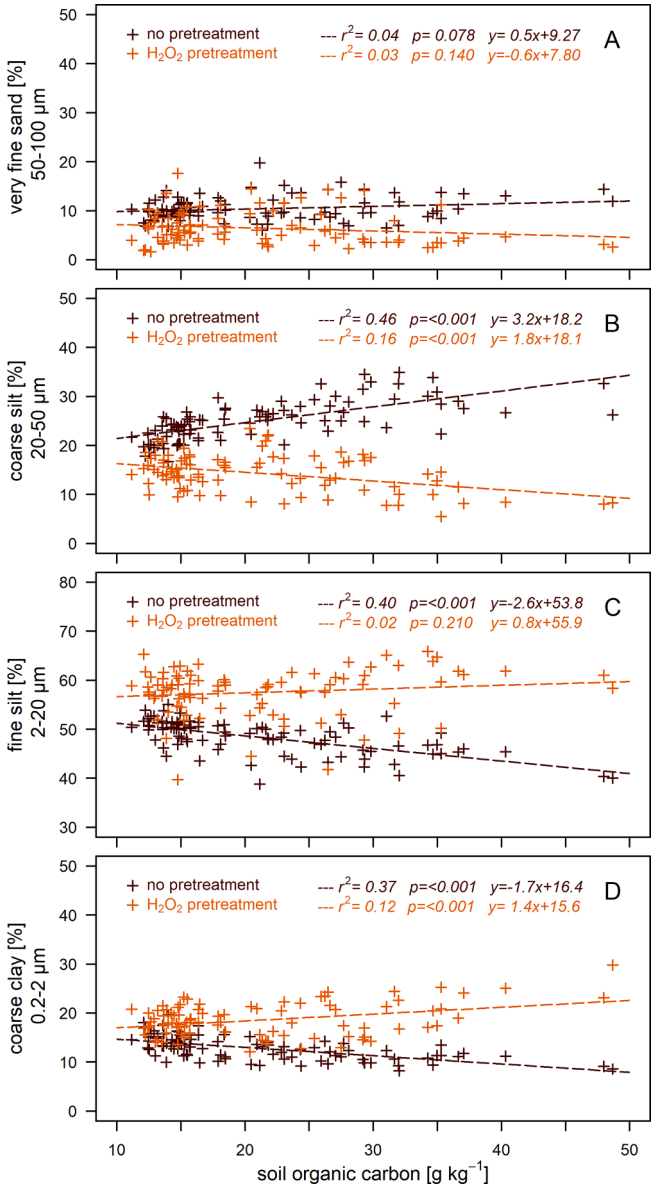

Fig. 7. Influence of soil organic carbon content [g kg^{-1}] on H_2O_2 pretreatment (+, dark brown) was compared with no pretreatment (+, light orange) for the texture subclasses (A) very fine sand (50–100 µm), (B) coarse silt (20–50 µm), (C) fine silt (2–20 µm) and (D) coarse clay (0.2–2 µm) in %. Trendline (– – –) and statistics for each pretreatment and texture subclasses are shown.

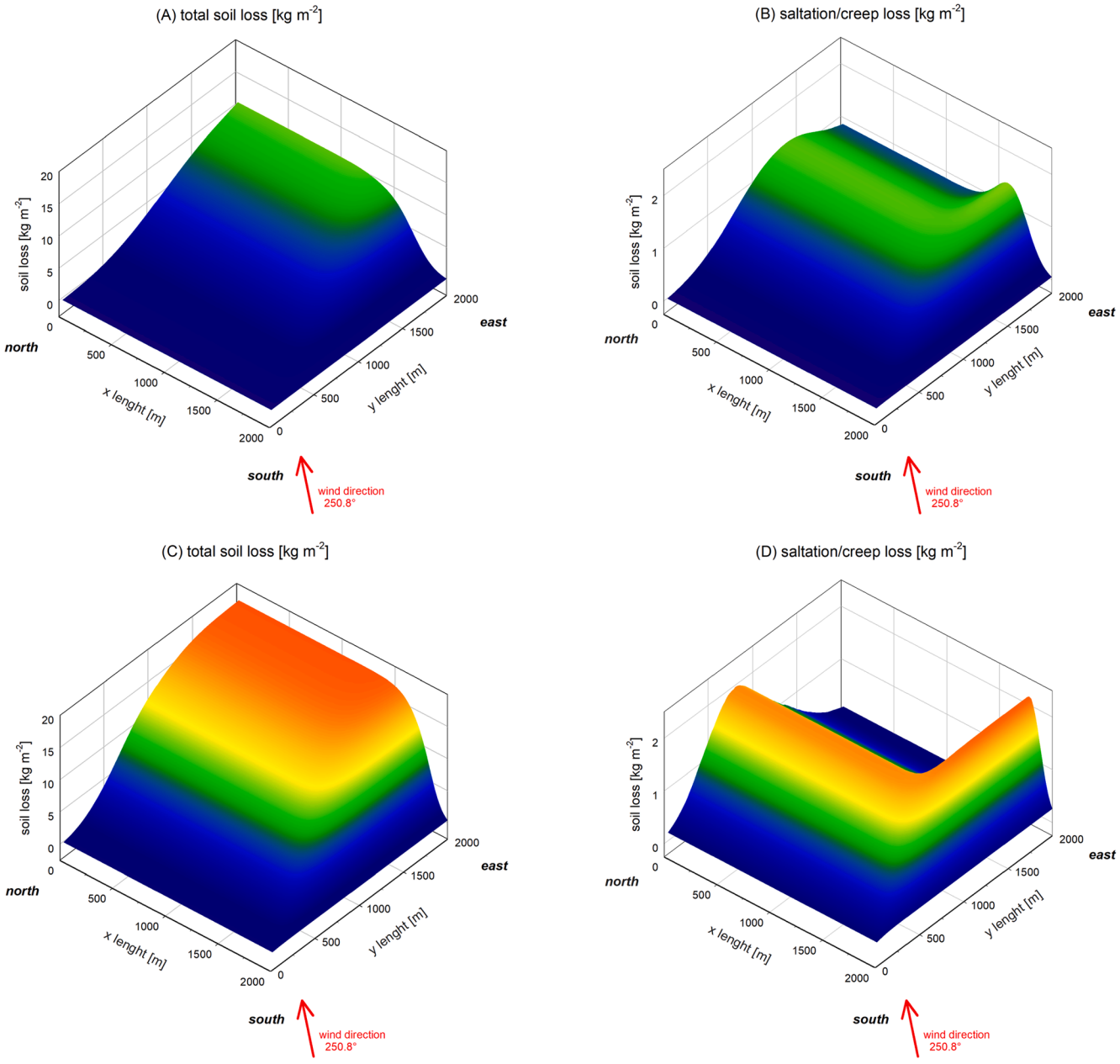

Fig. 8. Graphical visualisation of total soil loss [kg m^{-2}] (A and C) and saltation/creep soil loss [kg m^{-2}] (B and D) for the test field simulated by SWEEP. A and B show soil loss simulations based on laser diffraction analysis, including a hydrogen peroxide pretreatment (Table 1 and Table 2) if the geometric mean diameter is calculated with a pedotransfer function from the SWEEP user manual. C and D show soil loss simulations based on laser diffraction analysis, including a hydrogen peroxide pretreatment and independently measured GMD (Table 1 and Table 3).

4.2. Efficiency of pretreatments to remove organic matter

The distribution of Chernozems and Kastanozems from north to south reflects a declining humus gradient similar to the western Siberian steppe (Bischoff et al., 2018). Our results also agree with the organic carbon loss study in the Russian dry steppe caused by land-use changes from native ecosystems to arable fields (Illiger et al., 2019).

Mineral components, especially the silt and clay fraction, are strongly associated with organic matter. All samples pretreated with H_2O_2 showed dispersion of soil aggregates and an increasing amount of finer particles. Our results agree with the study of Di Stefano et al. (2010). They also measured a shift towards finer particles in PSD by LDA with H_2O_2 pretreatment, especially in the silt fraction.

Fisher et al. (2017) pretreated samples with sodium hypochlorite solution (NaClO) to remove organic matter and subsequently with HCl to remove carbonates. Using sodium hypochlorite differs from international standard methodologies but is suitable for their local Australian soils. They expected that the difference of the effect by NaClO + HCl pretreatment depends on the amount of organic carbon content. However, their results did not show a significant correlation between pretreatment and organic carbon content but showed a significant effect due to the soil type and therefore expected differences between no pretreatment and chemical pretreatment for different soil types. This supports our results of Chernozems and Kastanozems. The difference between no pretreatment and H_2O_2 pretreatment correlated with the organic carbon content and indicates that organic matter is likely the primary binding agent. Our results show that H_2O_2 pretreatment offers a complete dispersion for measuring PSD.

4.3. Pretreatments for laser diffraction analysis

Results of LDA assigned overall the same texture class in our study. Chemical pretreatment, soil type or land-use did not have an impact. On our test sites, chemical pretreatments for particle size analysis can be omitted if only the texture class is of interest. Even though sample preparation did affect particles within the silt fraction between 2 and 50 μm most severely, particles of the coarse and fine silt fractions are subjected to compensating effects. Changes in subclasses are hidden if they are not explicitly observed.

We agree with Fisher et al. (2017) that the advantages and disadvantages of using pretreatments for LDA for a broader range of soil types are warranted. In their study, the purpose of adapting a pretreatment for removing carbon seemed only of little purpose. Different effects were observed from pretreatment, but sample preparation generally decreased rather than increased the concordance correlation coefficient. Our results show similarities because only H_2O_2 pretreatment was efficient but did not change PSD severely. Additional pretreatments seem questionable despite the time-consuming preparation and potentially misleading results.

Laser diffraction has been increasingly applied for analysing PSD (Yang et al., 2019). It measures a 3-dimensional shape with a 1-dimensional parameter (Fisher et al., 2017) differently than the sieve and sedimentation method. Overall, LDA dismisses methodological disadvantages of the traditional sedimentation methods (Bittelli et al., 2019). It is questionable if the complete dispersion for particle size analysis is always necessary if measured by laser diffraction. Even though little is known about the possible effects of different pretreatments (Fisher et al., 2017), our results showed only minimal differences. For most soil types with a low and medium amount of organic binding material, a pretreatment seems nonessential if PSD is measured by laser diffraction.

4.4. Modelling effect of LDA pretreatments on wind erosion

The Wind Erosion Prediction System is a promising tool, and SWEEP can be used to estimate soil loss easily for single wind events in the dry steppe of Kazakhstan. Wind barriers were not present at the test site, even though Russia systematically introduced wind agroforestry to protect soils from erosion in the late nineteenth century (Chendev et al., 2015). Since 1991, the afforestation of agricultural land in Kazakhstan has usually been decreased because of political and economic change. In Losovoye, shelterbelts were partly cleared in the past because the trapped amount of snow caused gully erosion after melting.

Soil texture is a critical parameter for estimating wind erosion processes. However, particles without structure and binding agents do not occur under field conditions in the dry steppe's topsoil layer. Properties derived from particle sizes, such as dry aggregate size distribution and aggregate stability, have a considerable impact on wind erosion modelling results which can be changed by mechanical breakdown. Parameters regarding the actual size and distribution of aggregates in the field have a higher impact on SWEEP's output than soil texture parameters from LDA under the influence of different pretreatments. Suppose the texture-based parameters were derived and used as input, soil loss estimates were very diverse and ranged between 3.3 and 11.8 mm of topsoil depth. All estimates would be noticeable under field conditions. Chepil (1960) associated quantities of annual soil loss of around 37 t ha^{-1} to be distinctly visible.

Regarding particle size, the very fine sand fraction is the determining factor in wind erosion because of its lowest threshold (Shao, 2008). Our results of LDA showed low amounts of sand, including low amounts of very fine sand in general, and SWEEP predicted low saltation loss. Pretreatment of samples did not lead to a shift in soil texture class. Silt loam with a generally low amount of fine sand is not that susceptible to wind erosion from the perspective of size.

In our study, the consequences of chemical pretreatments for particle size analysis by LDA for modelling wind erosion did not differ, if the additional parameter GMD was independently measured. The SWEEP simulations from our test field are representable for our study area because averaged PSD data estimated similar soil losses. At the test field, topsoil loss was estimated less than 10 mm during the potentially strong wind event independent of LDA pretreatment. These potential soil losses are certainly overestimations, based on the maximum wind speeds as input data. However, with quantities of about 100 t ha^{-1}, they would cause considerable on- and off-site damage (Funk and Reuter, 2006).

Modelling results indicate that parameters derived from soil texture are more influential for wind erosion modelling than the texture itself. Therefore, deriving GMD from texture and binding agents with a pedotransfer function or a regression equation from the erodible fraction needs further validation (Fryrear et al., 1994; López et al., 2007; Rakkar et al., 2019). This is especially important for different dry steppe soil types, with a high aggregation potential at the microscale. New pedotransfer functions are required to derive soil parameters based on PSD with no pretreatment (Zimmermann and Horn, 2020) and for PSD data obtained by laser diffraction.

5. Conclusions

For particle size analysis of Chernozem and Kastanozem soils, an HCl pretreatment to dissolve carbonates should be avoided because it leads to incomplete dispersion or even an aggregation. An H_2O_2 pretreatment to remove organic binding material is sufficient. However, chemical pretreatments to remove binding agents for LDA did not significantly affect PSD in our study. Consequences for wind erosion modelling are major if texture-based parameters are derived by pedotransfer functions based on PSD and used as input data. In case independently measured GMD is available the consequences are minimal. Altogether, we conclude that derived properties from PSD by LDA require further investigation for dry steppe soils. A validation of the soil loss under field conditions with an in-situ experiment will be the next step.

Declaration of Competing Interest

The authors declare that they have no known competing financial interests or personal relationships that could have appeared to influence the work reported in this paper.

Acknowledgements

We highly appreciate the constructive comments from three anonymous reviewers and the editor regarding this manuscript. We thank the whole ReKKS Team and the Department of Geoecology and the Department of Soil Sciences and Soil Protection from the Martin Luther University Halle-Wittenberg (MLU). We are particularly grateful to Dorothee Kley (MLU), Olga Shibistova (Leibniz University, Hannover), and Tobias Meinel (Amazone, Nur-Sultan) for logistical assistance. Patrick Illiger (MLU) and Aleksey Prays (MLU), we thank for supporting fieldwork. We appreciate TOO Taynsha Astyk, TOO Fermer 2002, and the Barayev Center for their permission to take soil samples. We thank Michael von Hoff (MLU) for operating the laser diffraction analyser and Alexander Kaestner (Sympatec, Clausthal-Zellerfeld) for technical assistance. Thanks to Lisa Haselow (UFZ, Halle) for meteorological data. Last but not least, we especially acknowledge Klaus Kaiser (MLU) and Robert Mikutta (MLU), as well as Roger Funk (ZALF, Müncheberg), John Tatarko (USDA-ARS, Fort Collins), Markus Koch (Leibniz University, Hannover), Thomas Thienelt (MLU) and Muhammad Usman (MLU) for ideas, comments, and discussion.

Funding source

This study was conducted within the research project ReKKS (Innovative Solutions for Sustainable Agriculture and Climate Adaptation in the Dry Steppes of Kazakhstan and Southwestern Siberia) and funded by the German Federal Ministry of Education and Research (BMBF) - grant number: FKZ 01LZ1704B.

Appendix A

Table A1
Cumulated clay, silt and sand fractions under different pretreatments: (1) no pretreatment, (2) hydrochloric acid (HCl) pretreatment, (3) hydrochloric acid soluble compounds (HCl_{SC}) pretreatment, (4) hydrogen peroxide (H_2O_2) pretreatment, (5) sequential hydrogen peroxide and hydrochloric acid (H_2O_2 + HCl) pretreatment from a variety of land-use types at three test sites. Statistical significance ($p \leq 0.05$) between pretreatments for each test site is indicated by lower case letters.

test site	land-use type	clay [%] 0–2 µm					silt [%] 2–50 µm					sand [%] 50–2000 µm				
		(1)	(2)	(3)	(4)	(5)	(1)	(2)	(3)	(4)	(5)	(1)	(2)	(3)	(4)	(5)
Yasnaya Poljana	steppe	11.27^{b}	7.14^{b}	9.20^{b}	19.61^{a}	20.23^{a}	73.15^{a}	74.74^{a}	77.73^{a}	74.98^{a}	73.37^{a}	15.58^{b}	5.65^{a}	15.14^{b}	15.82^{b}	6.40^{a}
	pasture	10.45^{c}	6.72^{b}	9.97^{c}	16.10^{a}	20.55^{d}	78.11^{a}	78.29^{a}	80.01^{a}	77.61^{ab}	74.35^{b}	11.44^{b}	5.62^{a}	13.27^{b}	12.43^{b}	5.10^{a}
	diverse tillage	11.56^{b}	7.41^{b}	11.41^{b}	19.20^{a}	22.58^{a}	76.05^{ab}	70.37^{a}	78.27^{b}	75.07^{ab}	70.03^{a}	12.39^{ab}	10.43^{ab}	14.32^{a}	13.52^{ab}	7.39^{b}
Shortandy	steppe	12.70^{c}	6.91^{b}	10.66^{bc}	19.97^{a}	19.60^{a}	73.73^{ab}	70.69^{a}	76.50^{b}	73.98^{ab}	71.74^{ab}	13.57^{b}	9.34^{a}	16.60^{b}	15.35^{b}	8.67^{a}
	reduced tillage	12.65^{c}	6.04^{b}	9.83^{c}	20.76^{a}	19.35^{a}	77.74^{c}	72.85^{a}	81.09^{b}	78.81^{bc}	73.56^{a}	10.80^{c}	6.61^{a}	12.46^{b}	12.22^{bc}	6.510^{a}
Losovoye	steppe	10.68^{d}	6.56^{b}	13.87 ^{cd}	18.29^{a}	16.22^{ac}	66.80^{b}	58.51^{a}	68.61^{b}	64.66^{b}	58.10^{a}	22.53^{a}	23.20^{a}	24.83^{a}	21.47^{a}	25.68^{a}
	pasture	12.14^{c}	6.52^{b}	11.97^{c}	16.18^{a}	17.27^{a}	71.74^{ab}	74.03^{ab}	76.73^{a}	71.97^{ab}	69.86^{b}	16.11^{b}	9.78^{a}	16.75^{b}	16.07^{b}	12.87^{ab}
	diverse tillage	14.00^{d}	5.86^{b}	8.83^{c}	19.40^{a}	16.79^{ad}	72.69^{ab}	73.20^{a}	79.62^{b}	76.67^{ab}	69.19^{ab}	13.31^{b}	7.40^{a}	14.52^{b}	14.50^{b}	14.02^{b}
	deep tillage	15.76^{ac}	6.91^{b}	13.17^{c}	18.83^{a}	19.34^{a}	72.30^{a}	73.64^{a}	79.44^{b}	73.58^{a}	69.32^{a}	11.94^{ab}	7.53^{a}	13.66^{b}	13.26^{b}	11.34^{ab}
	no-tillage	15.56^{d}	5.54^{b}	11.85c	19.34^{a}	18.66^{a}	72.17^{a}	72.84^{a}	79.82^{b}	72.90^{a}	68.58^{a}	12.27^{b}	7.81^{a}	14.64^{b}	15.25^{b}	12.76^{b}
	reduced tillage	11.61^{c}	5.70^{b}	11.68^{c}	17.02^{a}	17.62^{a}	72.78^{ab}	70.50^{ab}	75.72^{a}	69.38^{ab}	67.18^{b}	15.61^{ab}	12.49^{a}	18.59^{ab}	18.94^{b}	15.21^{ab}
	fallow	13.67^{c}	6.19^{b}	11.20^{c}	17.91^{a}	19.76^{a}	74.84^{a}	74.20^{a}	79.92^{b}	75.39^{a}	70.33^{c}	11.48^{c}	7.89^{a}	13.89^{b}	13.42^{b}	9.91^{c}

Appendix B

Table B1
Parameters of physical–chemical analysis including particle size analysis with different pretreatments from two test sites and different land-use-types: (I) steppe, (II) pasture, (III) diverse tillage, (IV) deep tillage, (V) no-tillage, (VI) reduced tillage and (VII) fallow. Statistical significance ($p \leq 0.05$) between land-use-types is indicated by lower case letters. The Single-event Wind Erosion Evaluation Program (SWEEP) was applied to the deep tillage test site (IV).

Parameter		Yasnaya Poljana			Losovoye						
		(I)	(II)	(III)	(I)	(II)	(III)	(IV)	(V)	(VI)	(VII)
bulk density [g cm^{-3}]		1.02^{a}	1.06^{a}	0.98^{a}	1.17^{a}	1.12^{a}	1.12^{a}	1.09^{a}	1.11^{a}	1.06^{a}	1.08^{a}
total carbon [g kg^{-1}]		39.6^{a}	34.5^{ab}	31.8^{b}	21.5^{ab}	24.3^{a}	23.2^{a}	23.4^{a}	24.2^{a}	19.1^{b}	22.3^{ab}
total nitrogen [g kg^{-1}]		3.39^{a}	2.73^{ab}	2.57^{b}	1.88^{ab}	1.96^{a}	1.52^{b}	1.56^{b}	1.53^{b}	1.61^{ab}	1.73^{ab}
soil organic carbon [g kg^{-1}]		35.3^{a}	30.9^{a}	29.5^{a}	21.1^{b}	19.4^{ab}	13.7^{c}	14.5^{c}	13.7^{c}	15.2^{ac}	16.2^{ac}
calcium carbonate [g kg^{-1}]		36.5^{a}	30.0^{a}	19.3^{a}	2.8^{c}	41.2^{a}	78.7^{b}	74.2^{b}	88.0^{b}	32.7^{a}	50.9^{a}
particle size and sample preparation											
clay [%]	(1) no pretreatment	11.27^{a}	10.45^{a}	11.56^{a}	10.68^{b}	12.14^{ab}	14.00^{ac}	15.76^{c}	15.56^{c}	11.61^{ab}	13.68^{ac}
	(2) HCl pretreatment	7.14^{a}	6.72^{a}	7.41^{a}	6.56^{ab}	6.52^{ab}	5.86^{bc}	6.91^{a}	5.54^{c}	5.70^{bc}	6.19^{abc}
	(3) HCl_{SC} pretreatment	9.20^{a}	9.97^{a}	11.41^{a}	13.87^{a}	11.97^{a}	8.83^{b}	13.17^{a}	11.85^{a}	11.68^{ab}	11.20^{ab}
	(4) H_2O_2 pretreatment	19.61^{a}	16.10^{a}	19.20^{a}	18.29^{a}	16.18^{a}	19.40^{a}	18.83^{a}	19.34^{a}	17.02^{a}	17.91^{a}
	(5) H_2O_2 + HCl pretreatment	20.23^{a}	20.55^{a}	22.58^{a}	16.22^{a}	17.27^{a}	16.79^{a}	19.34^{a}	18.66^{a}	17.62^{a}	19.76^{a}
silt [%]	(1) no pretreatment	73.15^{b}	78.11^{a}	76.05^{ab}	66.80^{b}	71.74^{a}	72.69^{a}	72.30^{a}	72.17^{a}	72.78^{a}	74.84^{a}
	(2) HCl pretreatment	77.73^{a}	80.01^{a}	78.27^{a}	68.61^{d}	76.73^{ab}	79.62^{ac}	79.44^{ac}	79.82^{ac}	75.72^{b}	79.92^{c}
	(3) HCl_{SC} pretreatment	74.98^{a}	77.60^{a}	75.07^{a}	64.66^{c}	71.97^{ab}	76.67^{b}	73.58^{ab}	72.90^{ab}	69.38^{ac}	75.39^{b}
	(4) H_2O_2 pretreatment	74.74^{a}	78.29^{a}	70.37^{a}	58.51^{b}	74.03^{a}	73.20^{a}	73.64^{a}	72.84^{a}	70.50^{a}	74.20^{a}
	(5) H_2O_2 + HCl pretreatment	73.37^{a}	74.35^{a}	70.03^{a}	58.10^{b}	69.86^{a}	69.19^{a}	69.32^{a}	68.58^{a}	67.18^{a}	70.33^{a}
sand [%]	(1) no pretreatment	15.58^{a}	11.44^{a}	12.39^{a}	22.53^{c}	16.11^{a}	13.31^{ab}	11.94^{ab}	12.27^{ab}	15.61^{ab}	11.48^{b}
	(2) HCl pretreatment	15.14^{a}	13.27^{a}	14.32^{a}	24.83^{d}	16.75^{ab}	14.52^{ac}	13.66^{c}	14.64^{ac}	18.59^{b}	13.89^{ac}
	(3) HCl_{SC} pretreatment	15.82^{a}	12.43^{a}	13.52^{a}	21.47^{c}	16.07^{abc}	14.50^{ab}	13.26^{b}	15.25^{ab}	18.94^{ac}	13.42^{ab}
	(4) H_2O_2 pretreatment	5.65^{a}	5.62^{a}	10.43^{a}	23.20^{b}	9.78^{a}	7.40^{a}	7.53^{a}	7.81^{a}	12.49^{a}	7.89^{a}
	(5) H_2O_2 + HCl pretreatment	6.40^{ab}	5.10^{a}	7.39^{b}	25.68^{b}	12.87^{a}	14.02^{a}	11.34^{a}	12.76^{a}	15.21^{a}	9.91^{a}

References

Abbas, F., Hammad, H.M., Ishaq, W., Farooque, A.A., Bakhat, H.F., Zia, Z., Fahad, S., Farhad, W., Cerdà, A., 2020. A review of soil carbon dynamics resulting from agricultural practices. J. Environ. Manage. 268, 110319 https://doi.org/10.1016/j.jenvman.2020.110319.

Allmaras, R.R., Burwell, R.E., Larson, W.E., Holt, R.F., 1966. Total Porosity and Random Roughness of the Interrow Zone as Influenced by Tillage.

Almaganbetov, N., Grigoruk, V., 2008. Degradation of Soil in Kazakhstan: Problems and Challenges. In: Simeonov, L., Sargsyan, V. (Eds.), Soil Chemical Pollution, Risk Assessment, Remediation and Security. Springer, Netherlands, Dordrecht, pp. 309–320. https://doi.org/10.1007/978-1-4020-8257-3_27.

Bischoff, N., Mikutta, R., Shibistova, O., Dohrmann, R., Herdtle, D., Gerhard, L., Fritzsche, F., Puzanov, A., Silanteva, M., Grebennikova, A., Guggenberger, G., 2018. Organic matter dynamics along a salinity gradient in Siberian steppe soils. Biogeosciences 15, 13–29. https://doi.org/10.5194/bg-15-13-2018.

Bisutti, I., Hilke, I., Raessler, M., 2004. Determination of total organic carbon – an overview of current methods. TrAC, Trends Anal. Chem. 23, 716–726. https://doi.org/10.1016/j.trac.2004.09.003.

Bittelli, M., Andrenelli, M.C., Simonetti, G., Pellegrini, S., Artioli, G., Piccoli, I., Morari, F., 2019. Shall we abandon sedimentation methods for particle size analysis in soils? Soil Tillage Res. 185, 36–46. https://doi.org/10.1016/j.still.2018.08.018.

Bowker, M.A., Belnap, J., Bala Chaudhary, V., Johnson, N.C., 2008. Revisiting classic water erosion models in drylands: The strong impact of biological soil crusts. Soil Biol. Biochem. 40, 2309–2316. https://doi.org/10.1016/j.soilbio.2008.05.008.

Carroll, D., Starkey, H.C., 1971. Reactivity of Clay Minerals with Acids and Alkalies. Clays Clay Miner. 19, 321–333. https://doi.org/10.1346/CCMN.1971.0190508.

Chendev, Y., Sauer, T., Ramirez, G., Burras, C., 2015. History of East European Chernozem Soil Degradation; Protection and Restoration by Tree Windbreaks in the Russian Steppe. Sustainability 7, 705–724. https://doi.org/10.3390/su7010705.

Chepil, W.S., 1960. Conversion of Relative Field Erodibility to Annual Soil Loss by Wind. Soil Science Society of America Proceedings 143–145. https://doi.org/10.2136/sssaj1960.03615995002400020022x.

Conklin, A.R., Meinholtz, R., 2004. Field sampling: principles and practices in environmental analysis, Books in soils, plants, and the environment. Marcel Dekker, New York.

Di Stefano, C., Ferro, V., Mirabile, S., 2010. Comparison between grain-size analyses using laser diffraction and sedimentation methods. Biosyst. Eng. 106, 205–215. https://doi.org/10.1016/j.biosystemseng.2010.03.013.

Eckmeier, E., Gerlach, R., Gehrt, E., Schmidt, M.W.I., 2007. Pedogenesis of Chernozems in Central Europe — A review. Geoderma 139, 288–299. https://doi.org/10.1016/j.geoderma.2007.01.009.

FAO, 2006. Guidelines for soil description, 4th ed. ed. Food and Agriculture Organization of the United Nations (FAO), Rome. Available from: http://www.fao.org/3/a-a0541e.pdf.

FAO/UNESCO, 2007. The Digital Soil Map of the World, 1:5.000.000; Version 3.6. Food and Agriculture Organization of the United Nations, Rome, United Nations Educational, Scientific and Cultural Organization, Paris. Available from: http://www.fao.org/geonetwork/srv/en/metadata.show%3Fid=14116.

FAO, 2012. AQUASTAT Country profile - Kazakhstan. Food and Agriculture Organization of the United Nations (FAO), Rome. Available from: http://www.fao.org/3/ca0366en/CA0366EN.pdf.

FAO, 2017. Kazakhstan - Country fact sheet on food and agriculture policy trends - Kazakhstan.Food and Agriculture Organization of the United Nations (FAO), Rome. Available from: http://www.fao.org/3/a-i7676e.pdf.

Fisher, P., Aumann, C., Chia, K., O'Halloran, N., Chandra, S., 2017. Adequacy of laser diffraction for soil particle size analysis. PLoS ONE 12, e0176510. https://doi.org/10.1371/journal.pone.0176510.

Frühauf, M., Meinel, T., Schmidt, G., 2020. The Virgin Lands Campaign (1954–1963) Until the Breakdown of the Former Soviet Union (FSU): With Special Focus on Western Siberia. In: Frühauf, M., Guggenberger, G., Meinel, T., Theesfeld, I., Lentz, S. (Eds.), KULUNDA: Climate Smart Agriculture, Innovations in Landscape Research. Springer International Publishing, Cham, pp. 101–118. https://doi.org/10.1007/978-3-030-15927-6_8.

Fryrear, D.W., Krammes, C.A., Williamson, D.L., Zobeck, T.M., 1994. Computing the wind erodible fraction of soils.

Funk, R., Reuter, H.I., 2006. Wind Erosion. In: Boardman, J., Poesen, J. (Eds.), Soil Erosion in Europe. John Wiley & Sons, Ltd, Chichester, UK, pp. 563–582. https://doi.org/10.1002/0470859202.ch41.

Gardner, W.R., 1956. Representation of Soil Aggregate-Size Distribution by a Logarithmic-Normal Distribution. Soil Sci. Soc. Am. J. 20, 151–153. https://doi.org/10.2136/sssaj1956.03615995002000020003x.

Gee, G.W., Or, D., 2002. 2.4 Particle-Size Analysis. In: Dane, J.H., Topp, C.G. (Eds.), SSSA Book Series. Soil Science Society of America. https://doi.org/10.2136/sssabookser5.4.c12.

Green, D.W., Perry, R.H., 2007. Perry's Chemical Engineers' Handbook, Eighth ed. McGraw-Hill Professional Publishing, Blacklick, USA.

Hagen, L.J., 1991. A wind erosion prediction system to meet user needs. J. Soil Water Conserv. 46, 106–111.

Harris, I.C., Jones, P.D., Osborn, T., 2020. CRU TS4.04: Climatic Research Unit (CRU) Time-Series (TS) version 4.04 of high-resolution gridded data of month-by-month variation in climate (Jan. 1901- Dec. 2019). Available from: https://catalogue.ceda.ac.uk/uuid/89e1e34ec3554dc98594a5732622bce9.

Illiger, P., Schmidt, G., Walde, I., Hese, S., Kudrjavzev, A.E., Kurepina, N., Mizgirev, A., Stephan, E., Bondarovich, A., Frühauf, M., 2019. Estimation of regional soil organic carbon stocks merging classified land-use information with detailed soil data. Sci. Total Environ. 695, 133755 https://doi.org/10.1016/j.scitotenv.2019.133755.

ISO 10390, 2005. Soil quality - Determination of pH. International Organization for Standardization (ISO), Geneva.

ISO 10693, 1995. Soil quality - Determination of carbonate content - Volumetric method. International Organization for Standardization (ISO), Geneva.

ISO 11277, 2002. Soil quality - Determination of particle size distribution in mineral soil and material - Method by sieving and sedimentation. International Organization for Standardization (ISO), Geneva.

ISO 13320, 2009. Particle Size Analysis - Laser diffraction methods. International Organization for Standardization (ISO), Geneva.
ISO 14488, 2007. Particulate materials - Sampling and sample splitting for the determination of particulate properties. International Organization for Standardization (ISO), Geneva.
Jarrah, M., Mayel, S., Tatarko, J., Funk, R., Kuka, K., 2020. A review of wind erosion models: Data requirements, processes, and validity. CATENA 187, 104388. https://doi.org/10.1016/j.catena.2019.104388.
Keesstra, S.D., Bouma, J., Wallinga, J., Tittonell, P., Smith, P., Cerdà, A., Montanarella, L., Quinton, J.N., Pachepsky, Y., van der Putten, W.H., Bardgett, R.D., Moolenaar, S., Mol, G., Jansen, B., Fresco, L.O., 2016. The significance of soils and soil science towards realisation of the United Nations Sustainable Development Goals. SOIL 2, 111–128. https://doi.org/10.5194/soil-2-111-2016.
Kettler, T.A., Doran, J.W., Gilbert, T.L., 2001. Simplified Method for Soil Particle-Size Determination to Accompany Soil-Quality Analyses. Soil Sci. Soc. Am. J. 65, 849. https://doi.org/10.2136/sssaj2001.653849x.
Kroetsch, D., Wang, C., 2007. Particle Size Distribution. In: Carter, M., Gregorich, E. (Eds.), Soil Sampling and Methods of Analysis. Second Edition. CRC Press. https://doi.org/10.1201/9781420005271.
Larney, F., 2007. Dry-Aggregate Size Distribution. In: Carter, M., Gregorich, E. (Eds.), Soil Sampling and Methods of Analysis. Second Edition. CRC Press. https://doi.org/10.1201/9781420005271.
Li, J., Ma, X., Zhang, C., 2020. Predicting the spatiotemporal variation in soil wind erosion across Central Asia in response to climate change in the 21st century. Sci. Total Environ. 709 https://doi.org/10.1016/j.scitotenv.2019.136060.
López, M.V., de Dios Herrero, J.M., Hevia, G.G., Gracia, R., Buschiazzo, D.E., 2007. Determination of the wind-erodible fraction of soils using different methodologies. Geoderma 139, 407–411. https://doi.org/10.1016/j.geoderma.2007.03.006.
Mikutta, R., Kleber, M., Kaiser, K., Jahn, R., 2005. Review: Organic matter removal from soils using hydrogen peroxide, sodium hypochlorite, and disodium peroxodisulfate. Soil Sci. Soc. Am. J. 69, 120. https://doi.org/10.2136/sssaj2005.0120.
Moeys, J., 2018. The soil texture wizard: R functions for plotting, classifying, transforming and exploring soil texture data 104. Available from: https://cran.r-project.org/web/packages/soiltexture/vignettes/soiltexture_vignette.pdf.
Muhs, D.R., Prins, M., Machalett, B., 2014. Loess as a Quaternary paleoenvironmental indicator. PAGES Mag 22, 84–85. https://doi.org/10.22498/pages.22.2.84.
Pi, H., Sharratt, B., Feng, G., Lei, J., Li, X., Zheng, Z., 2016. Validation of SWEEP for creep, saltation, and suspension in a desert–oasis ecotone. Aeolian Res. 20, 157–168. https://doi.org/10.1016/j.aeolia.2016.01.006.
Prishchepov, A.V., Schierhorn, F., Dronin, N., Ponkina, E.V., Müller, D., 2020. 800 Years of Agricultural Land-use Change in Asian (Eastern) Russia. In: Frühauf, M., Guggenberger, G., Meinel, T., Theesfeld, I., Lentz, S. (Eds.), KULUNDA: Climate Smart Agriculture, Innovations in Landscape Research. Springer International Publishing, Cham, pp. 67–87. https://doi.org/10.1007/978-3-030-15927-6_6.
R Core Team, 2020. R: A language and environment for statistical computing. R Foundation for Statistical Computing, Vienna. Available from: https://www.r-project.org/.
RStudio Team, 2020. R: Integrated Development for R. RStudio, Boston. Available from: https://rstudio.com/products/rstudio/.
Rachkovskaya, E.I., Bragina, T.M., 2012. Steppes of Kazakhstan: Diversity and Present State. In: Werger, M.J.A., van Staalduinen, M.A. (Eds.), Eurasian Steppes. Ecological Problems and Livelihoods in a Changing World, Plant and Vegetation. Springer, Netherlands, Dordrecht, pp. 103–148. https://doi.org/10.1007/978-94-007-3886-7_3.
Rakkar, M.K., Blanco-Canqui, H., Tatarko, J., 2019. Predicting soil wind erosion potential under different corn residue management scenarios in the central Great Plains. Geoderma 353, 25–34. https://doi.org/10.1016/j.geoderma.2019.05.040.
Rawls, W.J., 1983. Estimating Soil Bulk Density from Particle Size Analysis and organic matter content. Soil Sci. 135, 123–125. https://doi.org/10.1097/00010694-198302000-00007.
Reyer, C.P.O., Otto, I.M., Adams, S., Albrecht, T., Baarsch, F., Cartsburg, M., Coumou, D., Eden, A., Ludi, E., Marcus, R., Mengel, M., Mosello, B., Robinson, A., Schleussner, C.-F., Serdeczny, O., Stagl, J., 2017. Climate change impacts in Central Asia and their implications for development. Reg Environ Change 17, 1639–1650. https://doi.org/10.1007/s10113-015-0893-z.
Rowley, M.C., Grand, S., Verrecchia, É.P., 2018. Calcium-mediated stabilisation of soil organic carbon. Biogeochemistry 137, 27–49. https://doi.org/10.1007/s10533-017-0410-1.
Schmidt, G., Illiger, P., Kudryavtsev, A.E., Bischoff, N., Bondarovich, A.A., Koshanov, N. A., Rudev, N.V., 2020. Physical Soil Properties and Erosion. In: Frühauf, M., Guggenberger, G., Meinel, T., Theesfeld, I., Lentz, S. (Eds.), KULUNDA: Climate Smart Agriculture. Springer International Publishing, Cham, pp. 155–166. https://doi.org/10.1007/978-3-030-15927-6_11.
Schulte, P., Lehmkuhl, F., Steininger, F., Loibl, D., Lockot, G., Protze, J., Fischer, P., Stauch, G., 2016. Influence of HCl pretreatment and organo-mineral complexes on laser diffraction measurement of loess–paleosol-sequences. CATENA 137, 392–405. https://doi.org/10.1016/j.catena.2015.10.015.
Shao, Y., 2008. Physics and modelling of wind erosion, 2. rev. & exp. In: Atmospheric and oceanographic sciences library, ed. ed Springer, S.l. https://doi.org/10.1007/978-1-4020-8895-7.
Six, J., Bossuyt, H., Degryze, S., Denef, K., 2004. A history of research on the link between (micro)aggregates, soil biota, and soil organic matter dynamics. Soil Tillage Res. 79, 7–31. https://doi.org/10.1016/j.still.2004.03.008.
Soil Science Division Staff, 2017. Soil survey manual, USDA Handbook 18., edited by C. Ditzler, K. Scheffe, and H. C. Monger. United States Department of Agriculture, Government Printing Office, Washington, D.C. Available from: https://www.nrcs.usda.gov/wps/portal/nrcs/detailfull/soils/ref/?cid=nrcs142p2_054262.
Sommer, R., Glazirina, M., Yuldashev, T., Otarov, A., Ibraeva, M., Martynova, L., Bekenov, M., Kholov, B., Ibragimov, N., Kobilov, R., Karaev, S., Sultonov, M., Khasanova, F., Esanbekov, M., Mavlyanov, D., Isaev, S., Abdurahimov, S., Ikramov, R., Shezdyukova, L., de Pauw, E., 2013. Impact of climate change on wheat productivity in Central Asia. Agric. Ecosyst. Environ. 178, 78–99. https://doi.org/10.1016/j.agee.2013.06.011.
Sonmez, S., Buyuktas, D., Okturen, F., Citak, S., 2008. Assessment of different soil to water ratios (1:1, 1:2.5, 1:5) in soil salinity studies. Geoderma 144, 361–369. https://doi.org/10.1016/j.geoderma.2007.12.005.
Stolbovoi, V., 2000. Soils of Russia: Correlated with the Revised Legend of the FAO Soil Map of the World and World Reference Base for Soil Resources, International Institute for Applied Systems Analysis, Laxenburg, Austria. Available from: http://pure.iiasa.ac.at/id/eprint/6111/1/RR-00-013.pdf.
Sympatec, 2019. Sympatec-Helos: Technische Spezifikationen. Sympatec GmbH, Clausthal-Zellerfeld.
Sympatec, 2012. HELOS/R: Central Unit - Operating Instructions. Sympatec GmbH, Clausthal-Zellerfeld.
Tatarko, J. (Ed.), 2008. Single-event Wind Erosion Evaluation program: SWEEP user manual draft (updated 6 October 2020). United States Department of Agriculture, Agricultural Research Service, Manhattan, KA, USA.
Tatarko, J., van Donk, S.J., Ascough, J.C., Walker, D.G., 2016. Application of the WEPS and SWEEP models to non-agricultural disturbed lands. Heliyon 2, e00215. https://doi.org/10.1016/j.heliyon.2016.e00215.
Tatarko, J., Wagner, L., Fox, F., 2019. The Wind Erosion Prediction System and its Use in Conservation Planning. In: Wendroth, O., Lascano, R.J., Ma, L. (Eds.), Advances in Agricultural Systems Modeling. American Society of Agronomy and Soil Science Society of America, Madison, WI, USA, pp. 71–101. https://doi.org/10.2134/advagricsystmodel8.2017.0021.
Teixeira, E.I., Fischer, G., van Velthuizen, H., Walter, C., Ewert, F., 2013. Global hot-spots of heat stress on agricultural crops due to climate change. Agric. For. Meteorol. 170, 206–215. https://doi.org/10.1016/j.agrformet.2011.09.002.
Tatarko, J. (Ed.), 2020. The Wind Erosion Prediction System (WEPS): Technical Documentation, USDA Agriculture Handbook 727. United States Department of Agriculture, Agricultural Research Service, Beltsville, MD, USA. Available from: https://www.ars.usda.gov/research/software/download/?softwareid=415.
UN, 2019. Sustainable development goals report 2019. United Nations (UN) publication issued by the Department of Economic and Social Affairs, New York. Available from: https://unstats.un.org/sdgs/report/2019.
Uspanov, U.U., Yevstifeyev, U.G., Storozhenko, D.M., Lobova, E.V., 1975. Soil Map of the Kazakh SSR 1:2.500.000.
Virto, I., Gartzia-Bengoetxea, N., Fernández-Ugalde, O., 2011. Role of Organic Matter and Carbonates in Soil Aggregation Estimated Using Laser Diffractometry. Pedosphere 21, 566–572. https://doi.org/10.1016/S1002-0160(11)60158-6.
WEF, 2020. The Global Risks Report 2020. World Economic Forum, Cologny. Available from: http://www3.weforum.org/docs/WEF_Global_Risk_Report_2020.pdf.
Wuddivira, M.N., Camps-Roach, G., 2007. Effects of organic matter and calcium on soil structural stability. Eur. J. Soil Sci. 58, 722–727. https://doi.org/10.1111/j.1365-2389.2006.00861.x.
Yang, Y., Wang, L., Wendroth, O., Liu, B., Cheng, C., Huang, T., Shi, Y., 2019. Is the Laser Diffraction Method Reliable for Soil Particle Size Distribution Analysis? Soil Sci. Soc. Am. J. 83, 276. https://doi.org/10.2136/sssaj2018.07.0252.
Zepner, L., Karrasch, P., Wiemann, F., Bernard, L., 2020. ClimateCharts.net – an interactive climate analysis web platform. Int. J. Digital Earth 1–19. https://doi.org/10.1080/17538947.2020.1829112.
Zimmermann, I., Horn, R., 2020. Impact of sample pretreatment on the results of texture analysis in different soils. Geoderma 371, 114379. https://doi.org/10.1016/j.geoderma.2020.114379.
Zobeck, T.M., Van Pelt, R.S., 2015. Wind Erosion. In: Hatfield, J.L., Sauer, T.J. (Eds.), Soil Management: Building a Stable Base for Agriculture. Soil Science Society of America, Madison, WI, USA, pp. 209–227. https://doi.org/10.2136/2011.soilmanagement.c14.